ISSN No: -2456-2165 https://doi.org/10.38124/ijisrt/26apr2380

Electrical Investigation of Leachate Plumes and Groundwater Pollution Using Integrated Geo-Electrical Methods and Physico-Chemical Analysis in Parts of Nasarawa State, North-Central Nigeria

Paul Amade Emmanuel[1]; Adeeko, T. O.[2]; Abu Mallam[2]; Farouq Ado Umar[3]

[1]Department of Physics, Bingham University, Karu, Nasarawa State
[2]Department of Physics, University of Abuja, Nigeria
[3]Industrial Safety & Environmental Technology Department, Petroleum Training Institute Effurun, Delta State Nigeria

Corresponding Author: Paul Amade Emmanuel*

Publication Date: 2026/05/09

Abstract: Groundwater resources in rapidly urbanizing settlements are increasingly threatened by uncontrolled solid-waste disposal and the migration of landfill leachate into shallow aquifers. This study evaluates the extent of subsurface and groundwater contamination associated with dumpsites within Karu Local Government Area, Nasarawa State, using an integrated geophysical–geochemilcal approach. A reconnaissance survey (field mapping, GPS positioning, and borehole inventory) guided the layout of resistivity profiles and sampling points. Electrical resistivity investigations comprised two-dimensional (2D) resistivity imaging (multiple-gradient array) and Vertical Electrical Sounding (VES) using the Schlumberger configuration, with inversion and modelling performed using WinResist to delineate lithologic layering, groundwater conditions, and conductive leachate plumes. Borehole water samples collected along established traverses were analysed for physicochemical parameters and major/trace elements, and contamination severity was evaluated using the Heavy Metal Pollution Index (HPI). Geophysical results consistently resolved three to four geoelectric layers interpreted as topsoil, sandy clay/clayey overburden, weathered basement, and fresh basement. Across the investigated dumpsites (including Angwa Adamu Kugbaru Ado, Auta Balefi, Tudun Wada, and Keffi), pronounced low-resistivity zones in the upper layers (typically within ~0–8 m, locally extending to ~18 m) contrast sharply with higher-resistivity control locations, indicating conductive leachate-impacted materials and potential pathways for lateral contaminant migration. The most intense anomalies occurred where very low resistivities were recorded within the near-surface and clayey horizons, suggesting elevated dissolved ionic content from waste-derived fluids. Water-quality results corroborate the geophysical interpretation, showing elevated electrical conductivity, suspended solids, nutrients (notably nitrate and phosphate), chloride, and multiple heavy metals at dump-impacted points, with several constituents exceeding guideline limits in some locations. Overall, the combined datasets indicate that shallow groundwater systems around the dumpsites are vulnerable to contamination, posing environmental and public-health risks. The study demonstrates the effectiveness of integrating resistivity methods with hydrochemical assessment for mapping leachate influence and identifying high-risk zones. It recommends improved waste containment and drainage control, protection/relocation of nearby water points, and routine groundwater monitoring to reduce exposure and support sustainable groundwater management in the study area.

How to Cite: Paul Amade Emmanuel; Adeeko, T. O.; Abu Mallam; Farouq Ado Umar (2026) Electrical Investigation of Leachate Plumes and Groundwater Pollution Using Integrated Geo-Electrical Methods and Physico-Chemical Analysis in Parts of Nasarawa State, North-Central Nigeria. *International Journal of Innovative Science and Research Technology*, 11(4), 3876-3905. https://doi.org/10.38124/ijisrt/26apr2380

ISSN No: -2456-2165 https://doi.org/10.38124/ijisrt/26apr2380

I. INTRODUCTION

Groundwater constitutes a critical component of global freshwater resources, particularly in regions experiencing rapid population growth and increasing demand for potable water. Its susceptibility to contamination is largely governed by its hydrological connectivity with the land surface and the physicochemical characteristics of the overlying saturated and unsaturated zones (Hasan et al., 2019). Among the major threats to groundwater quality is leachate infiltration from landfills and open dumpsites, a problem that has long been recognized in environmental studies (Ganiyu et al., 2015). In many developing countries, including Nigeria, solid wastes are frequently disposed of in unregulated sites such as abandoned excavations, valleys, and urban spaces, thereby increasing the risk of subsurface contamination.

To evaluate groundwater vulnerability, the DRASTIC model developed by the United States Environmental Protection Agency (USEPA) has been widely adopted due to its integrative approach to hydrogeological assessment (Aller et al., 1987; Miao et al., 2020; Rossetto et al., 2020; Bui et al., 2020). The model incorporates seven key parameters; depth to water, net recharge, aquifer media, soil media, topography, vadose zone impact, and hydraulic conductivity, which collectively determine the pollution potential of aquifers. These parameters are quantified using a system of ranges, ratings, and weights, allowing for site-specific evaluation and adaptability (Barbulescu, 2020). Despite the robustness of this framework, the effectiveness of groundwater protection remains limited in regions where landfill practices are poorly managed.

Landfill systems in developing countries often fall short of standard engineering requirements, resulting in shallow, unlined dumps that permit uncontrolled leachate migration (Gurrero et al., 2013). Such conditions facilitate the introduction of heavy metals and other contaminants into soils and aquifers, posing significant environmental and health risks (Olowookere et al., 2018; Atedhor, 2012). Even in cases where engineered landfills exist, studies have shown that they may still contribute to groundwater contamination under certain conditions (Seo, 2007). The cumulative effect of inadequate waste management, weak institutional frameworks, and financial limitations further exacerbates this problem in developing regions (Elaigwu et al., 2007; Pawlowska et al., 2000; Oyeku, 2010).

In Nigeria, the widespread practice of open dumping is driven by economic and technological constraints, as well as limited awareness of its environmental consequences (Adewole, 2009; Ako et al., 1990). This has led to increasing concerns regarding groundwater pollution, which has been reported in several parts of the country, including Niger State, where domestic waste disposal has significantly degraded groundwater quality (Rafiu and Mallam, 2016). Given that a large proportion of the population depends on groundwater for domestic use, the health implications of such contamination, particularly from heavy metals are considerable (Gurrero et al., 2013).

In response to these challenges, this study adopts an integrated methodological approach combining geo-electrical techniques and physicochemical analyses to assess groundwater quality in the vicinity of dumpsites in Nasarawa State, Nigeria. The study specifically focuses on delineating leachate plumes, evaluating groundwater contamination using heavy metal pollution indices, and establishing relationships between electrical resistivity and water quality parameters. By providing a comprehensive assessment of dumpsite-induced contamination, this research aims to contribute to improved groundwater resource management, support environmental policy formulation, and enhance decision-making processes related to land use and public health protection.

II. GEOLOGY OF THE STUDY AREA

Nasarawa State, located in the Middle Belt region of Nigeria between latitudes 7°45′–9°25′N and longitudes 7°–9°37′E, covers approximately 26,875.59 km² with a population of about 1.83 million (2006 census). Geologically, the area forms part of the Basement Complex of North-Central Nigeria and is predominantly underlain by the Younger Granite Complex. The lithology is broadly classified into three units: the undifferentiated migmatite complex of Archean to Proterozoic age, metavolcano-sedimentary rocks of Late Proterozoic age, and the Older Granite Complex (Pan-African Granites) of Late Precambrian to Lower Paleozoic age. These rock units have been extensively deformed and reworked during the Pan-African thermotectonic event, which significantly influenced their structural and geochemical characteristics (Oyawoye, 1972; Black et al., 1979; Ajibade et al., 1987; Rahaman, 1988).

III. GROUNDWATER OCCURRENCE IN BASEMENT COMPLEX ROCKS OF NIGERIA

Groundwater occurrence in the Basement Complex rocks of Nigeria is generally limited due to the predominance of hard, crystalline igneous and metamorphic formations, which exhibit low primary porosity and permeability. Consequently, water availability in these terrains depends largely on secondary features such as weathering and fracturing, creating significant hydrogeological challenges in both semi-arid and humid regions (Offodile, 1975; 1992; 2002). The Basement Complex is subdivided into key hydrogeological provinces, including the Older Granite–migmatite–gneiss complex, metasedimentary (schists, phyllites, and quartzites) units, and the Younger Granite complex. In the Older Granite and gneiss terrains, groundwater is typically confined to weathered overburden, with coarse granites yielding sandy aquifer materials, while feldspar-rich rocks weather into clayey formations that act as aquitards. The metasedimentary units exhibit variable groundwater potential, with quartzites and fractured pegmatites serving as relatively better aquifers compared to schists and phyllites. In contrast, the Younger Granite and associated fluvio-volcanic formations often present enhanced groundwater

ISSN No: -2456-2165 https://doi.org/10.38124/ijisrt/26apr2380

prospects due to extensive jointing, fracturing, and weathered zones, particularly within valley depressions where shallow aquifers are commonly exploited through boreholes and hand-dug wells. Overall, groundwater distribution in these terrains is highly heterogeneous and structurally controlled, emphasizing the importance of detailed hydrogeological and geophysical investigations for sustainable groundwater development (Offodile, 1992).

IV. METHODOLOGY

The study adopts an integrated methodological approach combining reconnaissance survey, geophysical investigation, and geochemical analysis to assess groundwater contamination in Karu L.G.A., Nasarawa State. A preliminary reconnaissance survey involving field mapping with compass/clinometer, measuring tape, GPS (Garmin GPS Map 7.8), and visual inspection is conducted to identify key hydrogeological features and existing boreholes within the study area. Electrical resistivity methods constitute the primary geophysical technique, employing two-dimensional (2D) resistivity imaging using the multiple-gradient array and vertical electrical sounding (VES) with the Schlumberger configuration to delineate subsurface lithology, groundwater conditions, and contaminant (leachate) plumes. Data acquisition is carried out using an ABEM Terrameter (SAS 1000/4000) with electrodes, connecting cables, clips, and power source, ensuring reliable subsurface resistivity measurements. A total of five traverses (100–150 m in length) are established across the dumpsite, while fourteen groundwater samples are collected from boreholes along these traverses for physicochemical analysis. The heavy metal pollution index (HPI) is applied to evaluate the extent of contamination, thereby enabling the integration of geophysical and geochemical datasets for comprehensive assessment of groundwater quality in the study area.

V. RESULTS AND DISCUSSIONS

➢ *Presentation of Results*

This study involved the acquisition of Vertical Electrical Sounding (VES) data across seven distinct areas in the study region to investigate subsurface characteristics and potential contamination from dumpsites. The areas surveyed were Angwa Adamu Kugbaru Ado (7^O 38’ 10.9” E , 9^O 2’ 26.2” N), Auta Balefi (7^O 34’ 20.87” E , 8^O 59’ 33.23” N), Tudun Wada (7^O 36’ 48.66”E , 9^O 23’ 5.69” N), Keffi (7^O 52’ 38.84” E , 8^O 50’ 48.93” N).

A total of 16 VES points were collected, with four VES points acquired at each of the seven areas. Specifically, three VES points were strategically positioned at each dumpsite to assess the subsurface properties potentially influenced by waste disposal activities, and one control VES point was established at a location sufficiently distant from the dumpsite to serve as a baseline for comparison.

The VES data were collected using the Schlumberger electrode array configuration, which is well-suited for delineating subsurface layering due to its sensitivity to vertical changes in electrical resistivity. These values were plotted against the corresponding electrode spacing (AB/2) to generate apparent resistivity curves. The curves were then matched against standard Schlumberger master curves to estimate initial layer parameters, including depth, thickness, and resistivity of subsurface layers. This curve-matching process provided a preliminary interpretation of the subsurface stratigraphy.

To refine the interpretation, the apparent resistivity data were modelled using WinResist software, a widely used tool for resistivity data inversion. The software iteratively adjusted the layer parameters to minimize the misfit between the observed and modeled resistivity data, producing detailed geoelectric models for each VES point. The resulting WinResist outputs, as illustrated in Figures 1 and 2, provide comprehensive information about the subsurface, including the number of geoelectric layers, the apparent resistivity of each layer, and the corresponding thickness and depth.

The general resistivity variation for H- and K-type curves $p_1 > p_2 < p_3$ and $p_1 < p_2 > p_3$, respectively, and we may be able to draw some conclusions about the relative values of p_1 and p_3. The A- and Q-type curves correspond to $p_1 < p_2 < p_3$ and $p_1 > p_2 > p_3$, respectively.

The inferred lithologies were determined based on the apparent resistivity values, which are indicative of the subsurface material properties. Resistivity ranges were correlated with known lithological characteristics typical of the study area, such as clay, sand, gravel, or weathered bedrock, and potential contamination zones were identified by comparing resistivity anomalies at dumpsite VES points with those at control points. For instance, lower resistivity values at dumpsite locations may suggest the presence of conductive contaminants, such as leachates, while higher resistivity values could indicate less altered or resistive materials like dry sand or bedrock. The detailed results, including specific resistivity values and their corresponding lithological interpretations, are presented in Figures 1, and 2 providing a clear visualization of the subsurface characteristics across the study areas.

This integrated approach, combining field data acquisition, curve matching, and software-based modelling, enabled a robust characterization of the subsurface environment, highlighting variations in lithology and potential contamination impacts associated with the dumpsites. The results form the basis for further discussion on the environmental implications of waste disposal practices in the study region.

➢ *WinResist Curve Graphs*

- *Angwa Adamu Kugbaru Ado*

The WinResist curve graph for Angwa Adamu Kugbaru Ado dumpsite VES 1, displayed in Figure 1, exhibits an HA-type curve with four layers. The apparent resistivity starts low at the surface (68.7 Ωm, 0–1.2 m), decreases slightly (22.8 Ωm, 1.2–4.3 m), increases significantly (348.2 Ωm, 4.3–10.8 m), and peaks sharply

ISSN No: -2456-2165 https://doi.org/10.38124/ijisrt/26apr2380

(11698.2 Ωm, 10.8–50 m). These also show HA-type curves, with VES 2 and VES 3 following similar trends: low resistivity in the upper layers (56.7–65.3 Ωm, 0–1.1 m; 25.5–28.6 Ωm, 1–5.7 m) and high resistivity deeper down (690.4–895.2 Ωm, 5.5–14.9 m; 10504–11811.7 Ωm, 9.7–50 m). The control point VES 4 has higher resistivity (103.5 Ωm, 0–1 m; 32.7 Ωm, 1–4.2 m; 617.3 Ωm, 4.2–15.1 m; 9105.1 Ωm, 15.1–50 m). The low resistivity in the upper layers of dumpsite curves suggests potential anomalies, while the control point's higher values indicate a more resistive subsurface.

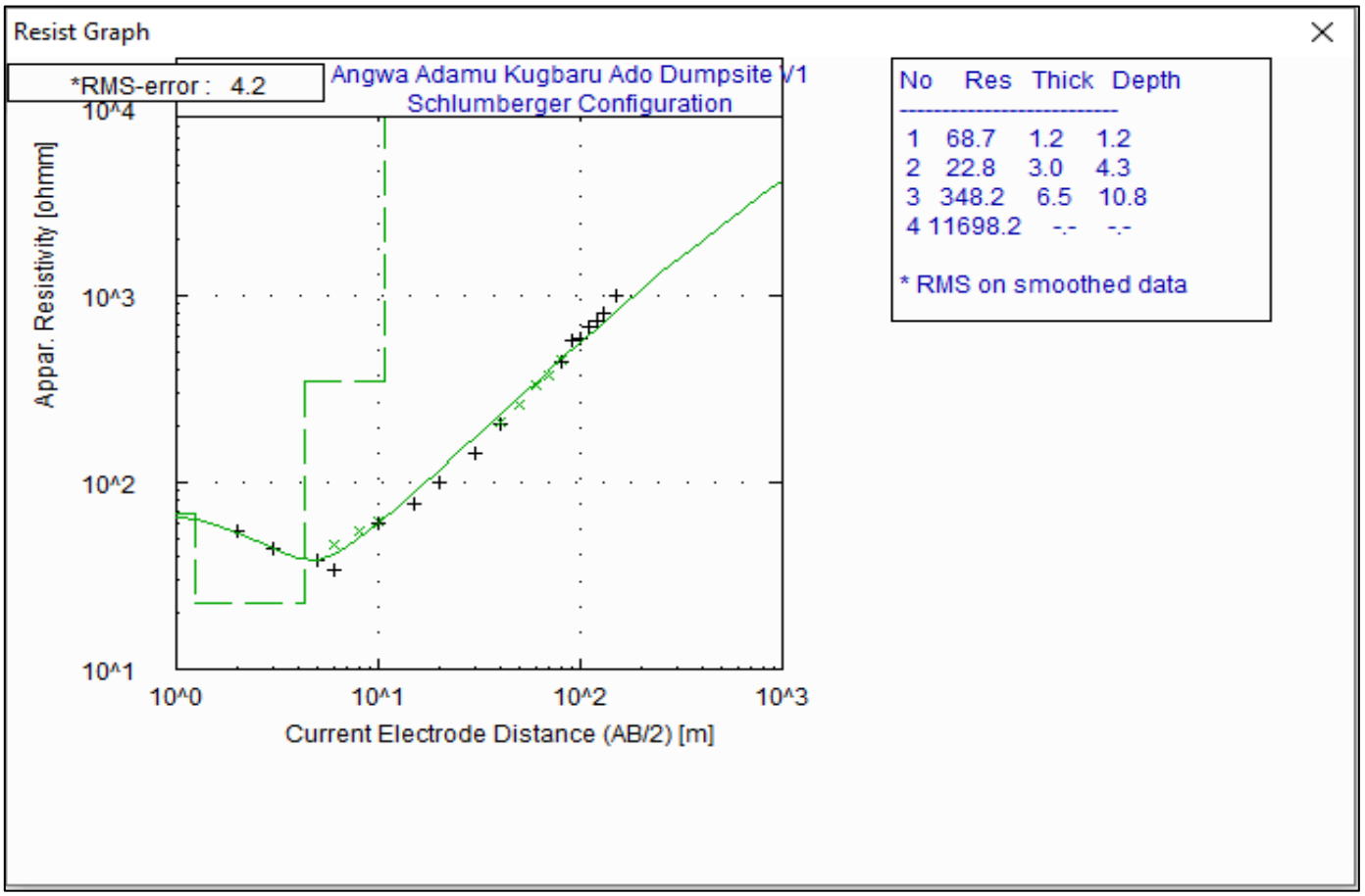

Fig 1 Vertical Electrical Sounding (VES) 1 curve at Angwa Adamu Kugbaru Ado Dumpsite, a four-layered model with an HA curve-type

- *Auta Balefi*

The WinResist curve for Auta Balefi dumpsite VES 1, shown in Figure 2, displays an AA-type curve with four layers, characterized by increasing resistivity: 22.3 Ωm (0–0.6 m), 29.6 Ωm (0.6–4.1 m), 179.9 Ωm (4.1–39.8 m), and 926.9 Ωm (39.8–60 m). Dumpsite VES 2 and VES 3 also exhibit AA-type curves with similar trends: low resistivity in the upper layers (16.7–17.4 Ωm, 0–0.4 m; 22.8–24.6 Ωm, 0.4–4.1 m) and increasing resistivity deeper (126.1–130 Ωm, 3.9–33.8 m; 758.6–871.7 Ωm, 31.9–60 m). The control point VES 4 (HA-type) shows higher resistivity: 139.7 Ωm (0–1.7 m), 53.8 Ωm (1.7–2.9 m), 107.8 Ωm (2.9–49.9 m), and 909 Ωm (49.9–60 m). The low resistivity in the upper layers of dumpsite curves indicates anomalies, contrasting with the control point's more resistive profile.

ISSN No: -2456-2165 https://doi.org/10.38124/ijisrt/26apr2380

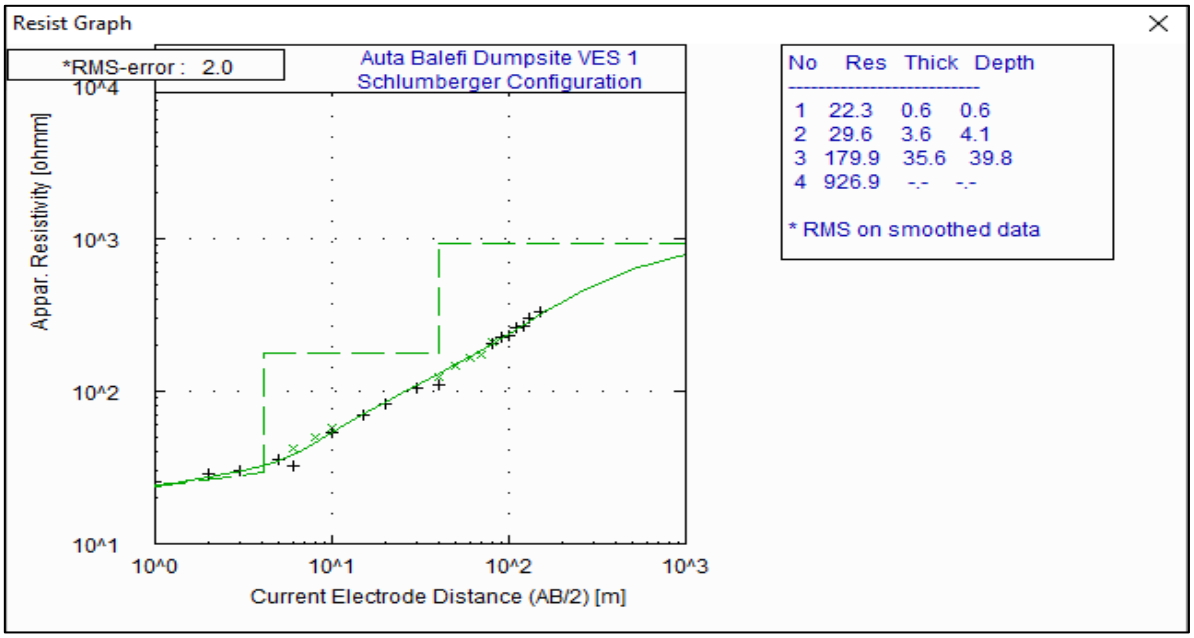

Fig 2 Vertical Electrical Sounding (VES) 1 curve at Auta Balefi Dumpsite, a four-layered model with an AA curve-type

- *Tudun Wada*

The WinResist curve for Tudun Wada dumpsite VES 1, presented in Figure 3, shows an HA-type curve with four layers: 53.8 Ωm (0–1.3 m), 9.1 Ωm (1.3–2.7 m), 538.5 Ωm (2.7–8.5 m), and 11428 Ωm (8.5–40 m). Dumpsite VES 2 and VES 3 exhibit AA-type curves with increasing resistivity: 6.2–7.5 Ωm (0–0.4 m), 11.8–15.8 Ωm (0.4–3.8 m), 81.1–554.2 Ωm (3.7–12.4 m), and 4150.5–5645.3 Ωm (5.7–40 m). The control point VES 4 (HA-type) has higher resistivity: 117.7 Ωm (0–0.8 m), 53.6 Ωm (0.8–5.4 m), 1196.5 Ωm (5.4–23.8 m), and 3106.6 Ωm (23.8–40 m). The extremely low resistivity in VES 2 and VES 3's upper layers (6.2–7.5 Ωm) suggests significant anomalies compared to the control point's resistive profile.

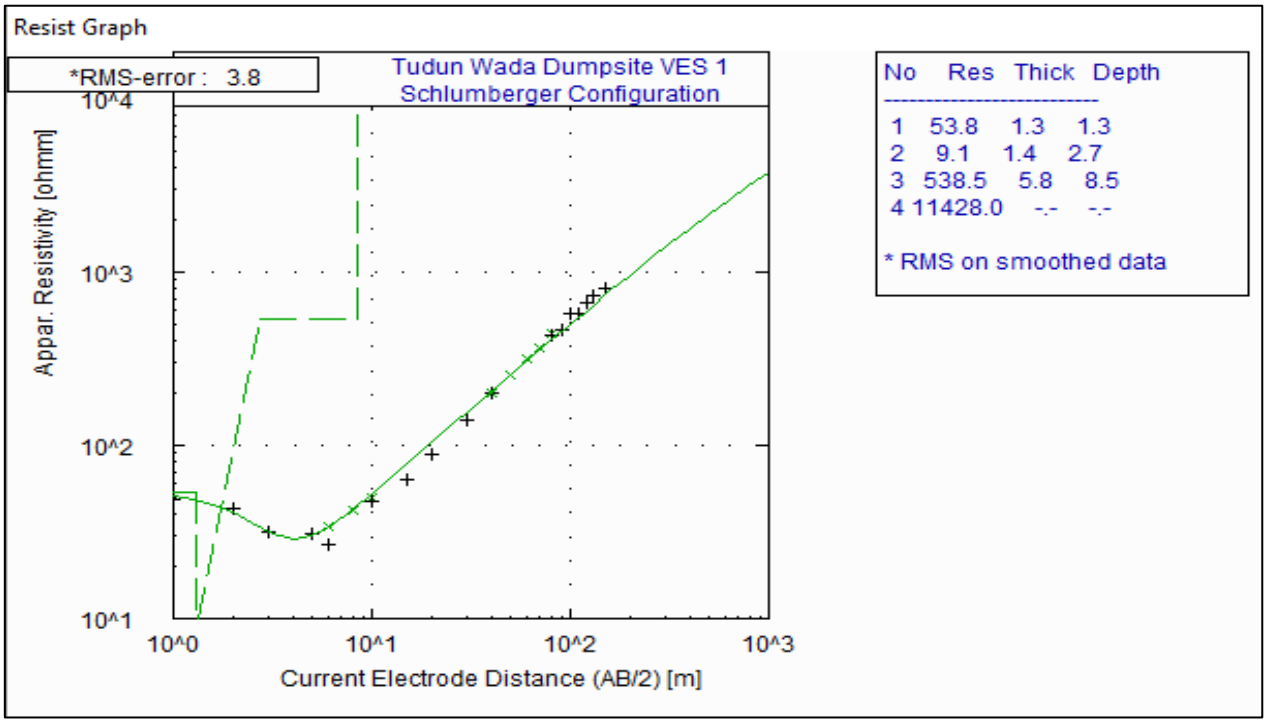

Fig 3 Vertical Electrical Sounding (VES) 1 curve at Tudun Wada Dumpsite, a four-layered model with an HA curve-type

- *Keffi*

The WinResist curve for Keffi dumpsite VES 1, illustrated in Figure 4, displays an HA-type curve with four layers: 20.8 Ωm (0–1.5 m), 5.6 Ωm (1.5–3.4 m), 1262.8 Ωm (3.4–27.1 m), and 3253.3 Ωm (27.1–40 m). Dumpsite VES 2 and VES 3 also show HA-type curves with low resistivity in the upper layers (15.7–23.2 Ωm, 0–3.6 m; 11.4–16.1 Ωm, 0.6–8 m) and higher resistivity deeper (21.4–685.5 Ωm, 1.9–26.5 m; 3361.7–4017.2 Ωm, 5–40 m). The control point VES 4 (QH-type) exhibits a distinct pattern: 195.8 Ωm (0–

ISSN No: -2456-2165 https://doi.org/10.38124/ijisrt/26apr2380

0.6 m), 93.5 Ωm (0.6–4.2 m), 43.1 Ωm (4.2–8.6 m), and 5783 Ωm (8.6–40 m). The low resistivity in the upper layers of dumpsite curves indicates anomalies, while the control point's QH-type curve with a resistivity drop and sharp increase suggests a unique subsurface structure.

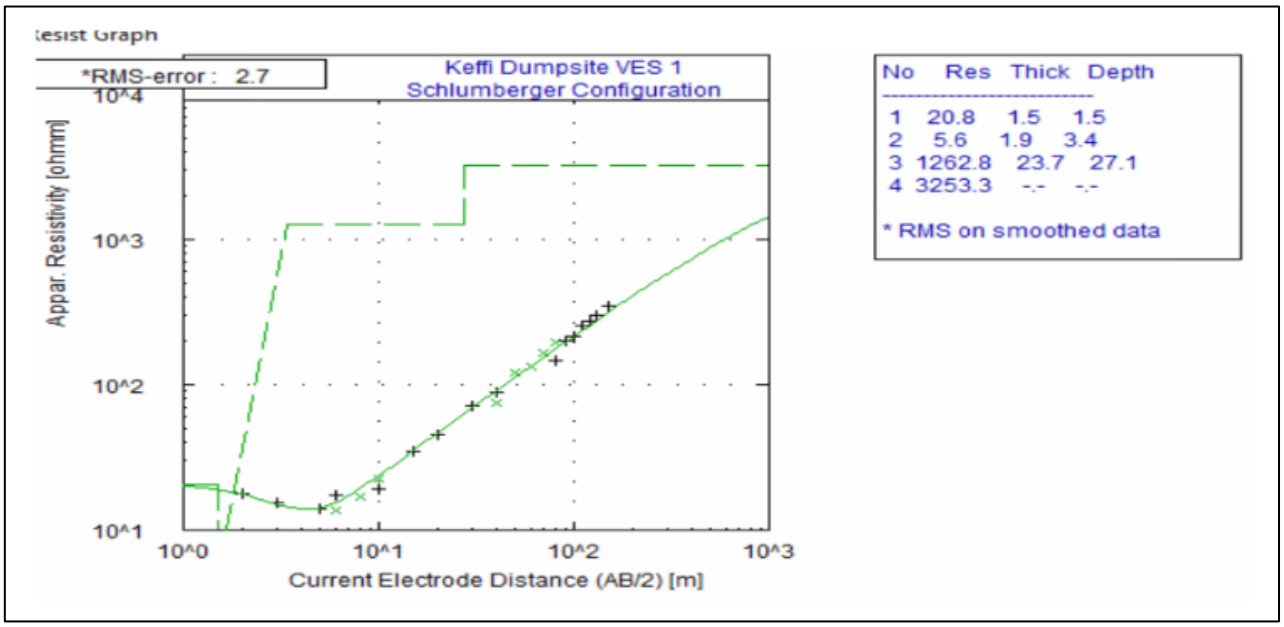

Fig 4 VES 1 at Keffi Dumpsite (four-layered model with an HA curve-type)

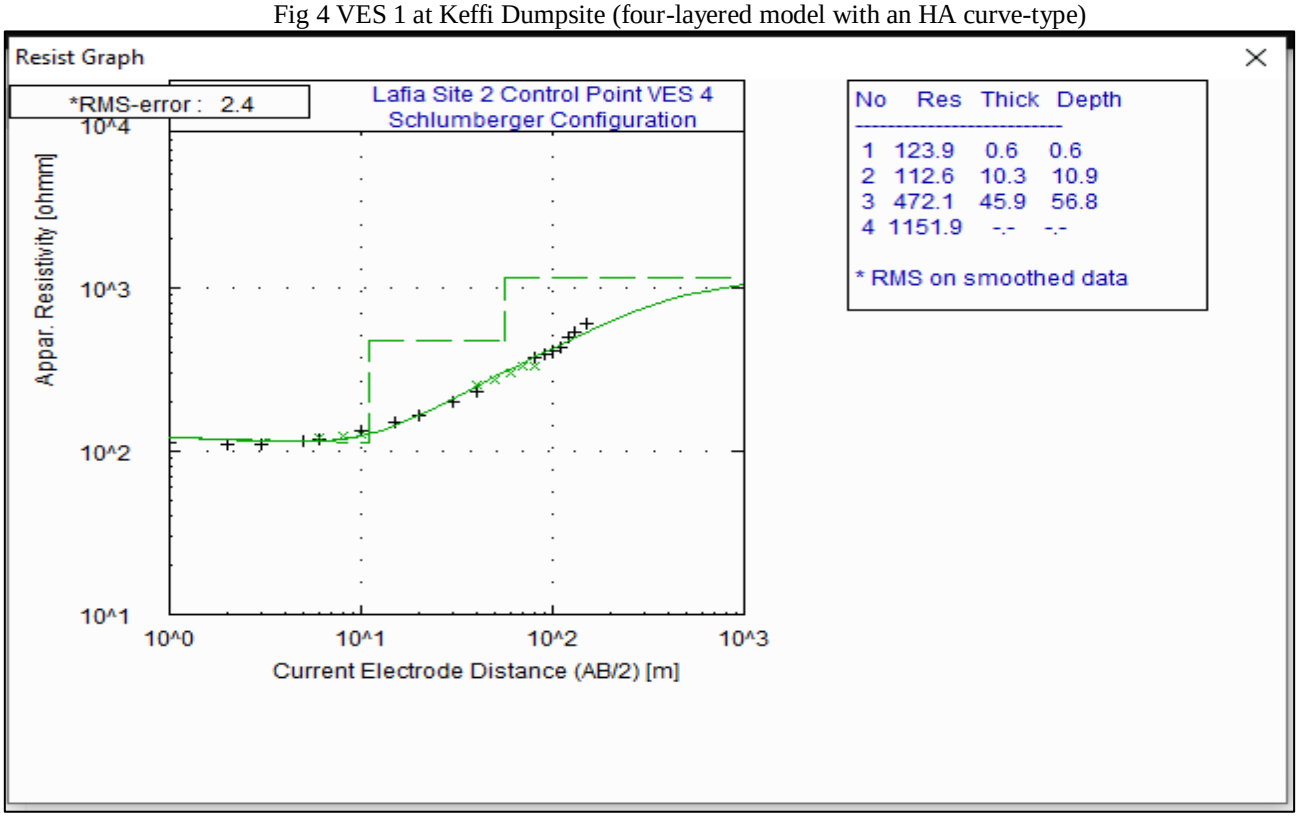

Fig 5 VES 4 Lafia Site 2 Control Point

➢ *Interpreted Geoelectric Log*

- *Angwa Adamu Kugbaru Ado*

The interpreted geoelectric log for Angwa Adamu Kugbaru Ado dumpsite VES 1, derived from WinResist modeling and presented in Figure 5, reveals four geoelectric layers with inferred lithology, emphasizing thickness and depth ranges. The layers are: Layer 1 (depth 0–1.2 m, thickness 1.2 m, 68.7 Ωm, topsoil), Layer 2 (depth 1.2–4.3 m, thickness 3.1 m, 22.8 Ωm, sandy clay), Layer 3 (depth 4.3–10.8 m, thickness 6.5 m, 348.2 Ωm, weathered basement), and Layer 4 (depth 10.8–50 m, thickness 39.2 m, 11698.2 Ωm, fresh basement). Dumpsite VES 2 and VES 3 show similar four-layer structures: VES 2 with Layer 1 (depth 0–1 m, thickness 1 m, 65.3 Ωm, topsoil), Layer 2 (depth 1–5.7 m, thickness 4.7 m, 28.6 Ωm, sandy clay),

ISSN No: -2456-2165 https://doi.org/10.38124/ijisrt/26apr2380

Layer 3 (depth 5.7–9.7 m, thickness 4 m, 895.2 Ωm, weathered basement), and Layer 4 (depth 9.7–50 m, thickness 40.3 m, 11811.7 Ωm, fresh basement); VES 3 with Layer 1 (depth 0–1.1 m, thickness 1.1 m, 56.7 Ωm, topsoil), Layer 2 (depth 1.1–5.5 m, thickness 4.4 m, 25.5 Ωm, sandy clay), Layer 3 (depth 5.5–14.9 m, thickness 9.4 m, 690.4 Ωm, weathered basement), and Layer 4 (depth 14.9–50 m, thickness 35.1 m, 10504 Ωm, fresh basement). The control point VES 4 has four layers: Layer 1 (depth 0–1 m, thickness 1 m, 103.5 Ωm, topsoil), Layer 2 (depth 1–4.2 m, thickness 3.2 m, 32.7 Ωm, sandy clay), Layer 3 (depth 4.2–15.1 m, thickness 10.9 m, 617.3 Ωm, weathered basement), and Layer 4 (depth 15.1–50 m, thickness 34.9 m, 9105.1 Ωm, fresh basement). Compared to the control point, dumpsite VES points show thinner upper layers (thickness 1–1.2 m vs. 1 m for topsoil; 3.1–4.7 m vs. 3.2 m for sandy clay) with significantly lower resistivity (56.7–68.7 Ωm vs. 103.5 Ωm in topsoil; 22.8–28.6 Ωm vs. 32.7 Ωm in sandy clay), suggesting potential pollution, while deeper layers have comparable thickness (35.1–40.3 m vs. 34.9 m for fresh basement) and resistivity.

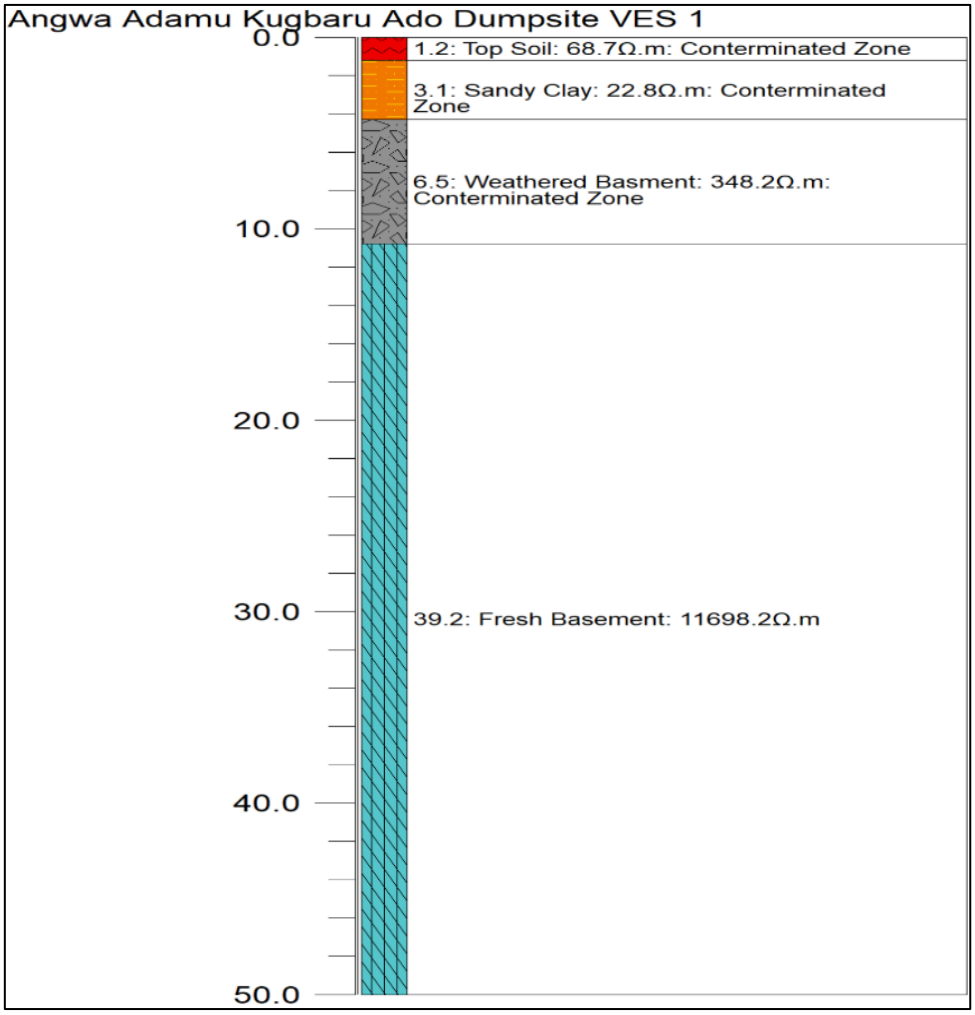

Fig 6 Geoelectric Log for Angwa Adamu Kugbaru Ado dumpsite VES 1

It revealed four layers: topsoil (0–1.2 m, 68.7 Ωm), sandy clay (1.2–4.3 m, 22.8 Ωm), weathered basement (4.3–10.8 m, 348.2 Ωm), and fresh basement (10.8–50 m, 11698.2 Ωm), indicating low resistivity in upper layers suggestive of pollution.

- *Auta Balefi*

The geoelectric log for Auta Balefi dumpsite VES 1, shown in Figure 6, reveals four layers with inferred lithology, emphasizing thickness and depth ranges: Layer 1 (depth 0–0.6 m, thickness 0.6 m, 22.3 Ωm, topsoil), Layer 2 (depth 0.6–4.1 m, thickness 3.5 m, 29.6 Ωm, sandy clay), Layer 3 (depth 4.1–39.8 m, thickness 35.7 m, 179.9 Ωm, weathered basement), and Layer 4 (depth 39.8–60 m, thickness 20.2 m, 926.9 Ωm, fresh basement). Dumpsite VES 2 and VES 3 show four layers: VES 2 with Layer 1 (depth 0–0.4 m, thickness 0.4 m, 16.7 Ωm, topsoil), Layer 2 (depth 0.4–4.1 m, thickness 3.7 m, 22.8 Ωm, sandy clay), Layer 3 (depth 4.1–33.8 m, thickness 29.7 m, 126.1 Ωm, weathered basement), and Layer 4 (depth 33.8–60 m, thickness 26.2 m, 758.6 Ωm, fresh basement); VES 3 with Layer 1 (depth 0–0.4 m, thickness 0.4 m, 17.4 Ωm, topsoil), Layer 2 (depth 0.4–3.9 m, thickness 3.5 m, 24.6 Ωm, sandy clay), Layer 3 (depth 3.9–31.9 m, thickness 28 m, 130 Ωm, weathered basement), and Layer 4 (depth 31.9–60 m, thickness 28.1 m, 871.7 Ωm, fresh basement). The control point VES 4 has four layers: Layer 1 (depth 0–1.7 m, thickness 1.7 m, 139.7 Ωm, topsoil), Layer 2 (depth 1.7–2.9

ISSN No: -2456-2165 https://doi.org/10.38124/ijisrt/26apr2380

m, thickness 1.2 m, 53.8 Ωm, sandy clay), Layer 3 (depth 2.9–49.9 m, thickness 47 m, 107.8 Ωm, weathered basement), and Layer 4 (depth 49.9–60 m, thickness 10.1 m, 909 Ωm, fresh basement). Dumpsite VES points have thinner upper layers (thickness 0.4–0.6 m vs. 1.7 m for topsoil; 3.5–3.7 m vs. 1.2 m for sandy clay) with significantly lower resistivity (16.7–22.3 Ωm vs. 139.7 Ωm in topsoil; 22.8–29.6 Ωm vs. 53.8 Ωm in sandy clay), suggesting pollution, while deeper layers show comparable resistivity but varying thickness (20.2–28.1 m vs. 10.1 m for fresh basement).

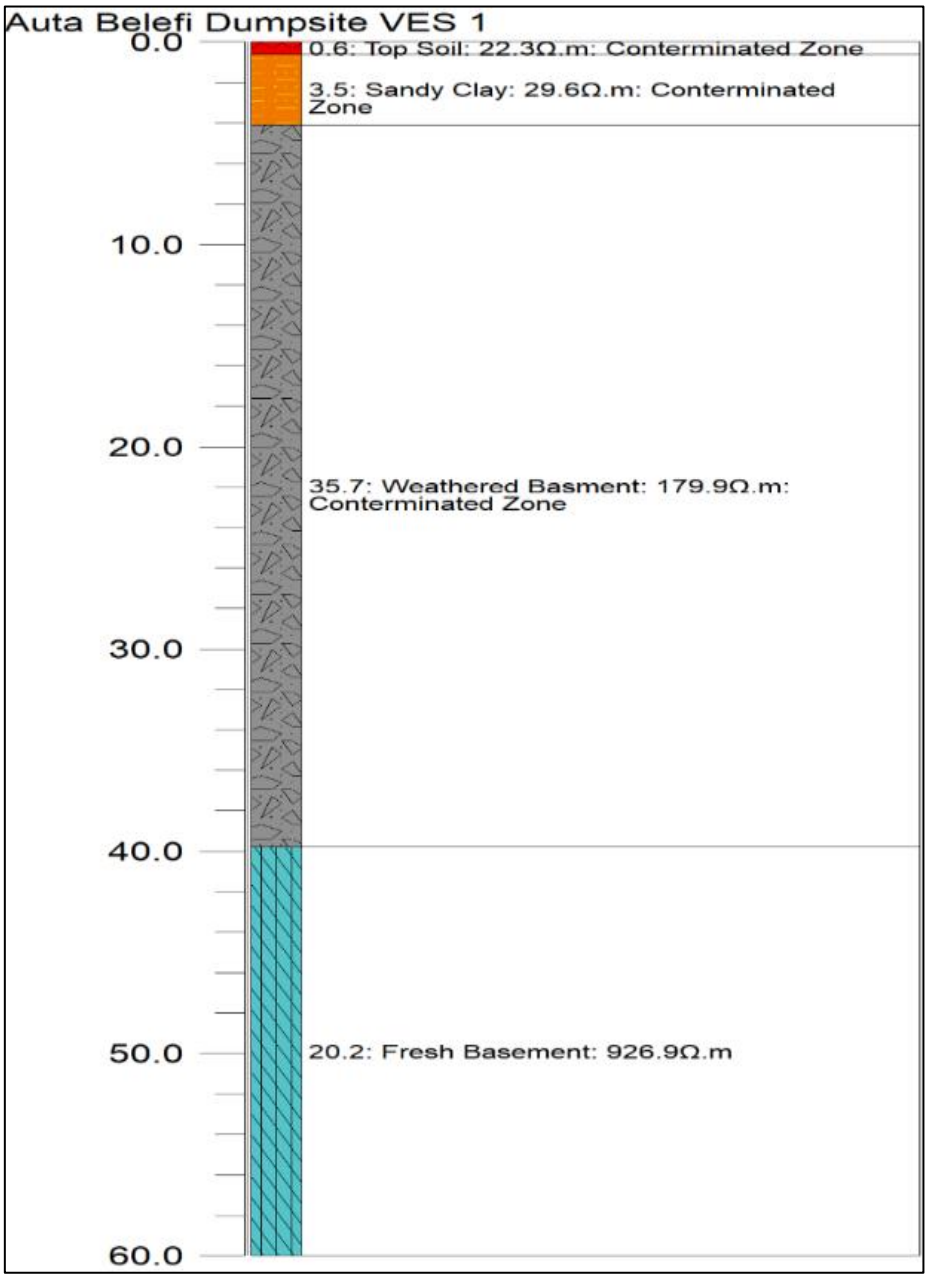

Fig 7 Geoelectric log for Auta Balefi dumpsite VES 1

It reveals four layers: topsoil (0–0.6 m, 22.3 Ωm), sandy clay (0.6–4.1 m, 29.6 Ωm), weathered basement (4.1–39.8 m, 179.9 Ωm), and fresh basement (39.8–60 m, 926.9 Ωm), with low upper-layer resistivity indicating potential pollution.

- *Tudun Wada*

The geoelectric log for Tudun Wada dumpsite VES 1, presented in Figure 7, shows four layers with inferred lithology, emphasizing thickness and depth ranges: Layer 1 (depth 0–1.3 m, thickness 1.3 m, 53.8 Ωm, topsoil), Layer 2 (depth 1.3–2.7 m, thickness 1.4 m, 9.1 Ωm, sandy clay), Layer 3 (depth 2.7–8.5 m, thickness 5.8 m, 538.5 Ωm, weathered basement), and Layer 4 (depth 8.5–40 m, thickness 31.5 m, 11428 Ωm, fresh basement). Dumpsite VES 2 and VES 3 have four layers: VES 2 with Layer 1 (depth 0–0.4 m, thickness 0.4 m, 7.5 Ωm, topsoil), Layer 2 (depth 0.4–3.8 m, thickness 3.4 m, 15.8 Ωm, sandy clay), Layer 3 (depth 3.8–5.7 m, thickness 1.9 m, 81.1 Ωm, weathered basement), and Layer 4 (depth 5.7–40 m, thickness 34.3 m, 4150.5 Ωm, fresh basement); VES 3 with Layer 1 (depth 0–0.4 m, thickness 0.4 m, 6.2 Ωm, topsoil),

ISSN No: -2456-2165 https://doi.org/10.38124/ijisrt/26apr2380

Layer 2 (depth 0.4–3.7 m, thickness 3.3 m, 11.8 Ωm, sandy clay), Layer 3 (depth 3.7–12.4 m, thickness 8.7 m, 554.2 Ωm, weathered basement), and Layer 4 (depth 12.4–40 m, thickness 27.6 m, 5645.3 Ωm, fresh basement). The control point VES 4 has four layers: Layer 1 (depth 0–0.8 m, thickness 0.8 m, 117.7 Ωm, topsoil), Layer 2 (depth 0.8–5.4 m, thickness 4.6 m, 53.6 Ωm, sandy clay), Layer 3 (depth 5.4–23.8 m, thickness 18.4 m, 1196.5 Ωm, weathered basement), and Layer 4 (depth 23.8–40 m, thickness 16.2 m, 3106.6 Ωm, fresh basement). Dumpsite VES points have thinner upper layers (thickness 0.4–1.3 m vs. 0.8 m for topsoil; 1.4–3.4 m vs. 4.6 m for sandy clay) with much lower resistivity (6.2–53.8 Ωm vs. 117.7 Ωm in topsoil; 9.1–15.8 Ωm vs. 53.6 Ωm in sandy clay), with VES 2 and VES 3 notably low (6.2–7.5 Ωm in topsoil), indicating potential pollution.

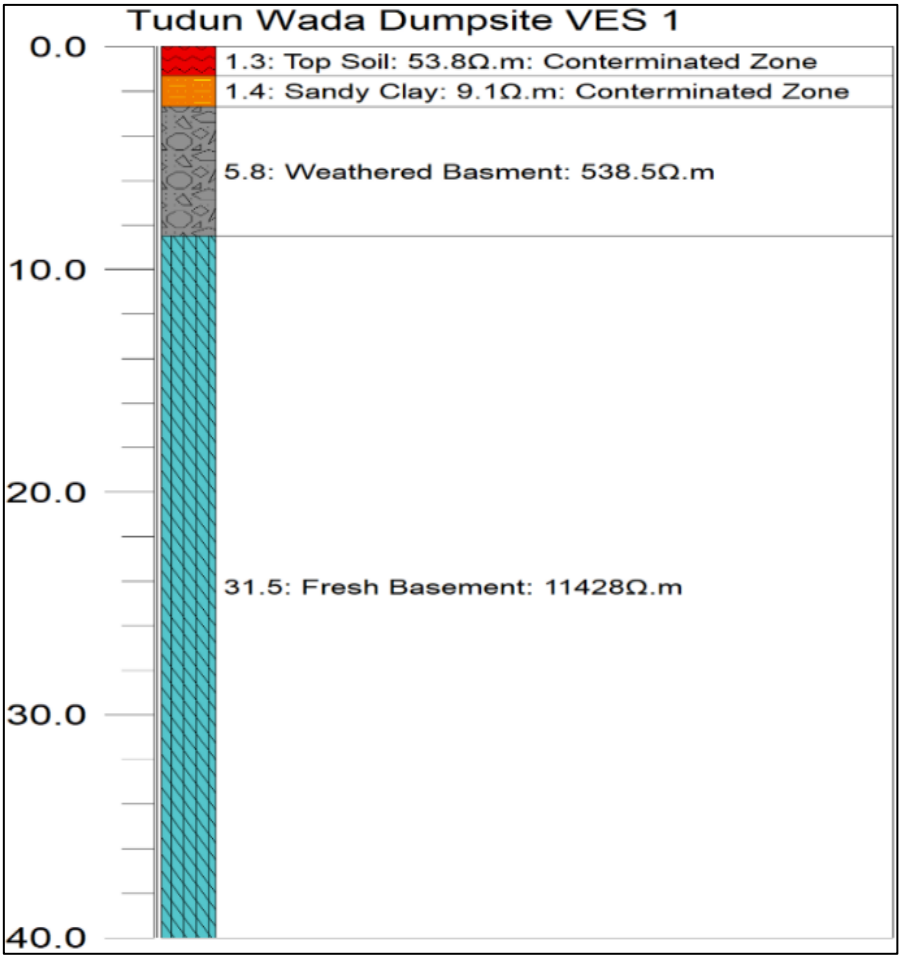

Fig 8 Geoelectric Log for Tudun Wada dumpsite VES 1

Displays four layers: topsoil (0–1.3 m, 53.8 Ωm), sandy clay (1.3–2.7 m, 9.1 Ωm), weathered basement (2.7–8.5 m, 538.5 Ωm), and fresh basement (8.5–40 m, 11428 Ωm), with low resistivity in sandy clay suggesting pollution.

- *Keffi*

The geoelectric log for Keffi dumpsite VES 1, shown in Figure 8, reveals four layers with inferred lithology, emphasizing thickness and depth ranges: Layer 1 (depth 0–1.5 m, thickness 1.5 m, 20.8 Ωm, topsoil), Layer 2 (depth 1.5–3.4 m, thickness 1.9 m, 5.6 Ωm, sandy clay), Layer 3 (depth 3.4–27.1 m, thickness 23.7 m, 1262.8 Ωm, fresh basement), and Layer 4 (depth 27.1–40 m, thickness 12.9 m, 3253.3 Ωm, fresh basement). Dumpsite VES 2 has four layers: Layer 1 (depth 0–0.6 m, thickness 0.6 m, 15.7 Ωm, topsoil), Layer 2 (depth 0.6–1.9 m, thickness 1.3 m, 11.4 Ωm, sandy clay), Layer 3 (depth 1.9–5 m, thickness 3.1 m, 21.4 Ωm, weathered basement), and Layer 4 (depth 5–40 m, thickness 35 m, 4017.2 Ωm, fresh basement); VES 3 has three layers: Layer 1 (depth 0–3.6 m, thickness 3.6 m, 23.2 Ωm, topsoil), Layer 2 (depth 3.6–8 m, thickness 4.4 m, 16.1 Ωm, sandy clay), and Layer 3 (depth 8–40 m, thickness 32 m, 3361.7 Ωm, fresh basement). The control point VES 4 has four layers: Layer 1 (depth 0–0.6 m, thickness 0.6 m, 195.8 Ωm, topsoil), Layer 2 (depth 0.6–4.2 m, thickness 3.6 m, 93.5 Ωm, sandy clay), Layer 3 (depth 4.2–8.6 m, thickness 4.4 m, 43.1 Ωm, clay), and Layer 4 (depth 8.6–40 m, thickness 31.4 m, 5783 Ωm, fresh basement). Dumpsite VES points have thinner upper layers (thickness 0.6–3.6 m vs. 0.6 m for topsoil; 1.3–4.4 m vs. 3.6 m for sandy clay) with significantly lower resistivity (15.7–23.2 Ωm vs. 195.8 Ωm in topsoil; 5.6–16.1 Ωm vs. 93.5 Ωm in sandy clay), suggesting pollution, while deeper layers show comparable thickness and resistivity.

ISSN No: -2456-2165 https://doi.org/10.38124/ijisrt/26apr2380

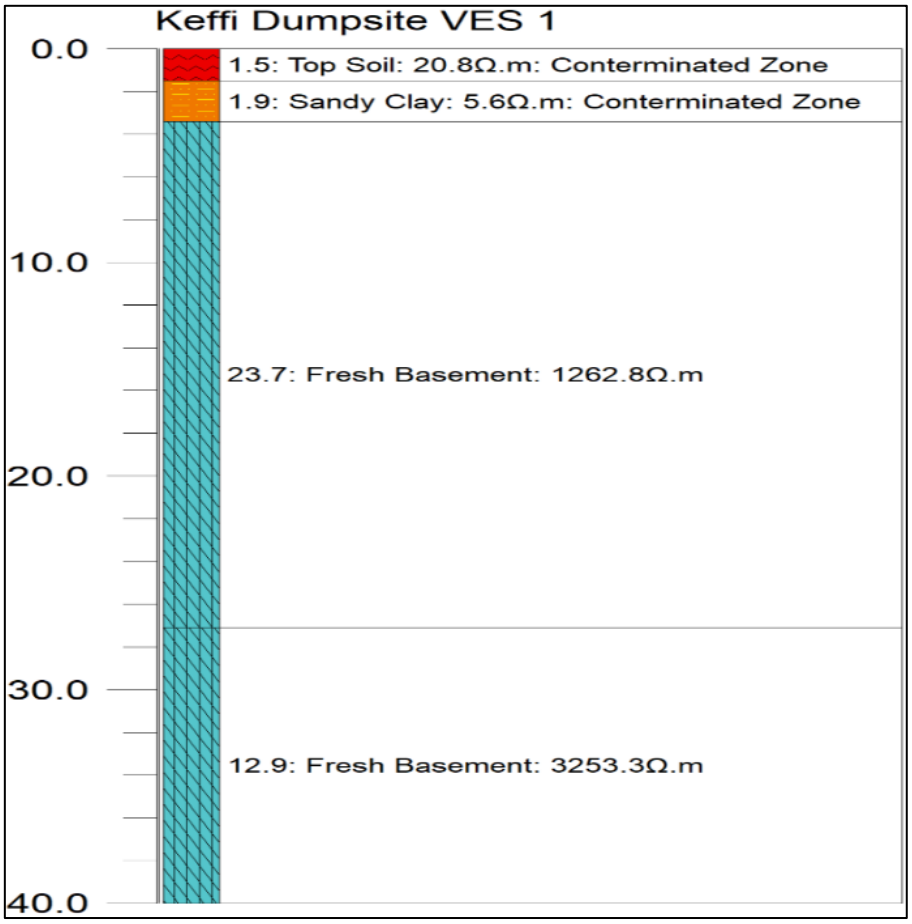

Fig 9 Geoelectric log for Keffi dumpsite VES 1

The figure above revealed four layers: topsoil (0–1.5 m, 20.8 Ωm), sandy clay (1.5–3.4 m, 5.6 Ωm), fresh basement (3.4–27.1 m, 1262.8 Ωm), and fresh basement (27.1–40 m, 3253.3 Ωm), with very low sandy clay resistivity indicating significant pollution.

➢ *2D Geoelectric and Hole-to-Hole Lithological Models*

- *Angwa Adamu Kugbaru Ado*

The 2D lithological model and hole-to-hole section for the Angwa Adamu Kugbaru Ado dumpsite (A to A' profile, 50 m total depth) are constructed from VES 1–3, positioned at 0 m (VES 1), 15 m (VES 2), and 30 m (VES 3), as shown in hole-to-hole section (Figure 9) and the geoelectric section (Figure 9). These sections connect the VES points to provide a lateral view of subsurface variations across the 30 m profile. The model identifies four lithological units based on apparent resistivity correlations: topsoil (56.7–68.7 Ωm, depth 0–1.2 m, thickness 1–1.2 m), sandy clay (22.8–28.6 Ωm, depth 1–5.7 m, thickness 3.1–4.7 m), weathered basement (348.2–895.2 Ωm, depth 4.3–14.9 m, thickness 4–9.4 m), and fresh basement (10504–11811.7 Ωm, depth 9.7–50 m, thickness 35.1–40.3 m). Resistivity ranges were correlated with lithology using standard geophysical interpretations: low resistivity (5–100 Ωm) for topsoil and sandy clay indicates conductive, potentially saturated or contaminated sediments; moderate resistivity (100–1000 Ωm) for weathered basement reflects partially weathered rock; and high resistivity (>1000 Ωm) for fresh basement signifies unweathered, resistive bedrock.

Compared to the control point VES 4 (topsoil 103.5 Ωm, depth 0–1 m, thickness 1 m; sandy clay 32.7 Ωm, depth 1–4.2 m, thickness 3.2 m; weathered basement 617.3 Ωm, depth 4.2–15.1 m, thickness 10.9 m; fresh basement 9105.1 Ωm, depth 15.1–50 m, thickness 34.9 m), dumpsite VES points exhibit significantly lower resistivity in the upper layers (56.7–68.7 Ωm vs. 103.5 Ωm in topsoil; 22.8–28.6 Ωm vs. 32.7 Ωm in sandy clay), suggesting contamination likely from leachate infiltration. The lowest resistivity at VES 3 (56.7 Ωm in topsoil, 25.5 Ωm in sandy clay) indicates a potential contamination hotspot at 30 m along the profile. Spatially, the topsoil maintains consistent thickness (1–1.2 m), while the sandy clay layer thickens slightly from 3.1 m at VES 1 to 4.7 m at VES 2, and the weathered basement thickens from 6.5 m at VES 1 to 9.4 m at VES 3, suggesting a deepening of weathered material toward the profile's end. The low-resistivity sandy clay layer (22.8–28.6 Ωm) extends laterally across the 30 m profile, forming a conductive zone that facilitates pollutant migration, potentially affecting shallow groundwater. The fresh basement's high resistivity (up to 11811.7 Ωm at VES 2) and substantial thickness (35.1–40.3 m) act as an impermeable barrier, limiting deeper pollutant migration. This configuration suggests that contaminants are likely confined to the upper 5.7 m, with significant implications for remediation efforts targeting shallow layers.

ISSN No: -2456-2165 https://doi.org/10.38124/ijisrt/26apr2380

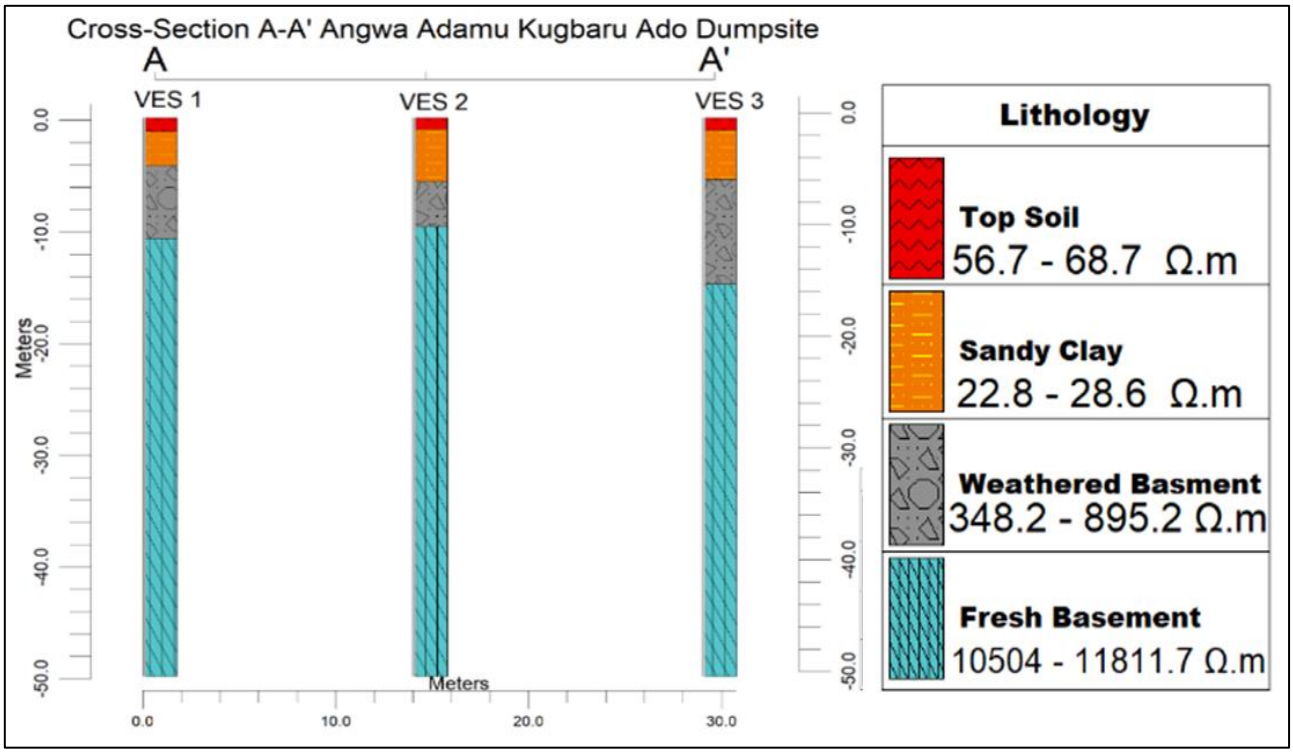

Fig 10 Hole-to-Hole

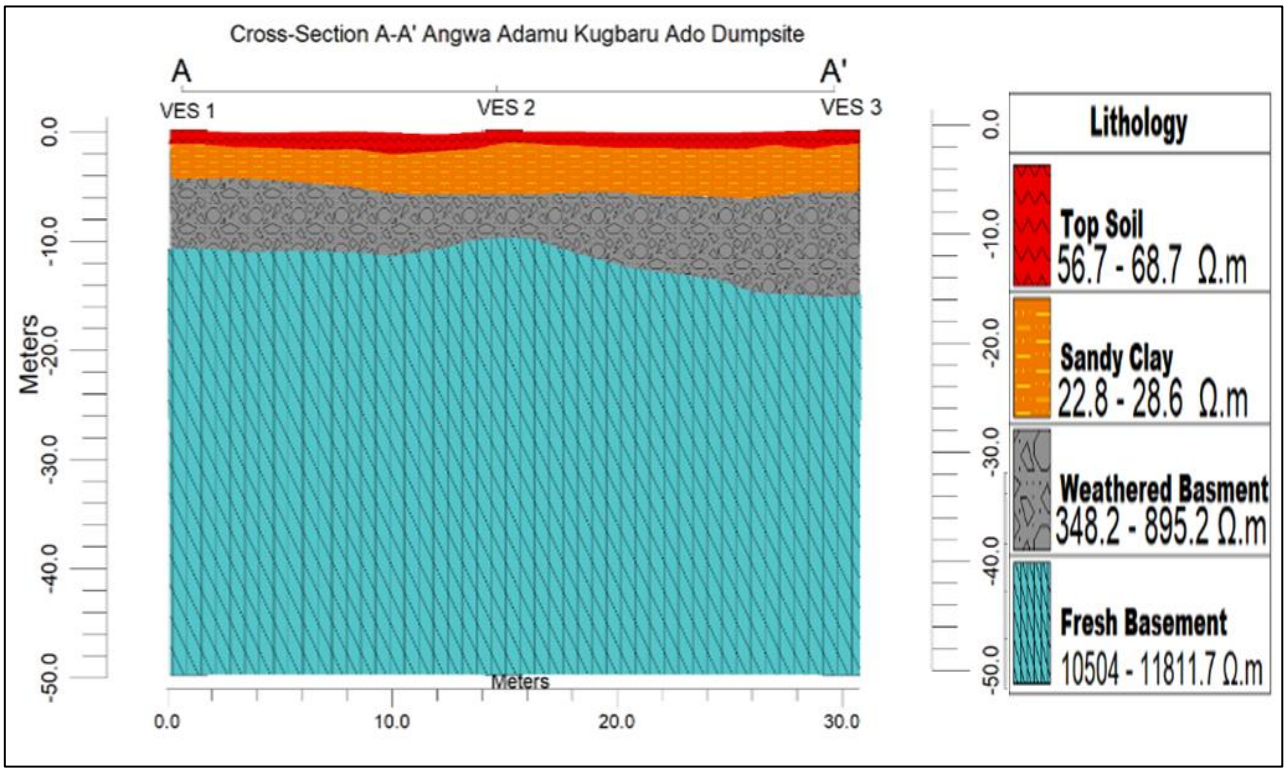

Fig 11 Geoelectric Section and lithological model Of Profile A to A' Angwa Adamu Kugbaru Ado Dumpsite

The profile A-A’ shows the geoelectric sections at 50 m depth for Angwa Adamu Kugbaru Ado dumpsite; topsoil (0–1.2 m, 56.7–68.7 Ωm), sandy clay (1–5.7 m, 22.8–28.6 Ωm), weathered basement (4.3–14.9 m, 348.2–895.2 Ωm), and fresh basement (9.7–50 m, 10504–11811.7 Ωm), with low-resistivity upper layers indicating potential contamination across the 30 m profile.

- *Auta Balefi*

The 2D lithological model and hole-to-hole section for the Auta Balefi dumpsite (B to B' profile, 60 m total depth), with VES 1 at 0 m, VES 2 at 15 m, and VES 3 at 30 m, are depicted in Figures 11 (geoelectric section) and 12 (hole-to-hole section). The model delineates four lithological units: topsoil (16.7–22.3 Ωm, depth 0–0.6 m, thickness 0.4–0.6 m), sandy clay (22.8–29.6 Ωm, depth 0.4–4.1 m, thickness

ISSN No: -2456-2165 https://doi.org/10.38124/ijisrt/26apr2380

3.5–3.7 m), weathered basement (126.1–179.9 Ωm, depth 3.9–39.8 m, thickness 28–35.7 m), and fresh basement (758.6–926.9 Ωm, depth 31.9–60 m, thickness 20.2–28.1 m). Resistivity correlations indicate conductive topsoil and sandy clay (5–100 Ωm) likely due to contamination or moisture, weathered basement (100–1000 Ωm) as partially altered rock, and fresh basement (>1000 Ωm) as unweathered bedrock. Compared to the control point VES 4 (topsoil 139.7 Ωm, depth 0–1.7 m, thickness 1.7 m; sandy clay 53.8 Ωm, depth 1.7–2.9 m, thickness 1.2 m; weathered basement 107.8 Ωm, depth 2.9–49.9 m, thickness 47 m; fresh basement 909 Ωm, depth 49.9–60 m, thickness 10.1 m), dumpsite VES points show significantly lower resistivity in the topsoil (16.7–22.3 Ωm) and sandy clay (22.8–29.6 Ωm), with the weathered basement (126.1–179.9 Ωm) also lower than typical, suggesting pollutant infiltration.

Spatially, the topsoil remains thin (0.4–0.6 m), while the weathered basement thickens significantly from 29.7 m at VES 2 to 35.7 m at VES 1, indicating deeper weathering at the profile's start. The low-resistivity topsoil and sandy clay layers extend across the 30 m profile, creating a continuous conductive zone that likely facilitates lateral pollutant migration, particularly toward VES 2 (16.7 Ωm in topsoil). The fresh basement's moderate resistivity (758.6–926.9 Ωm) and thickness (20.2–28.1 m) suggest a partial barrier to deeper migration, though the thick weathered basement (up to 35.7 m) may allow some pollutant penetration. This configuration indicates a high risk of shallow groundwater contamination, with remediation needing to focus on the upper 4.1 m.

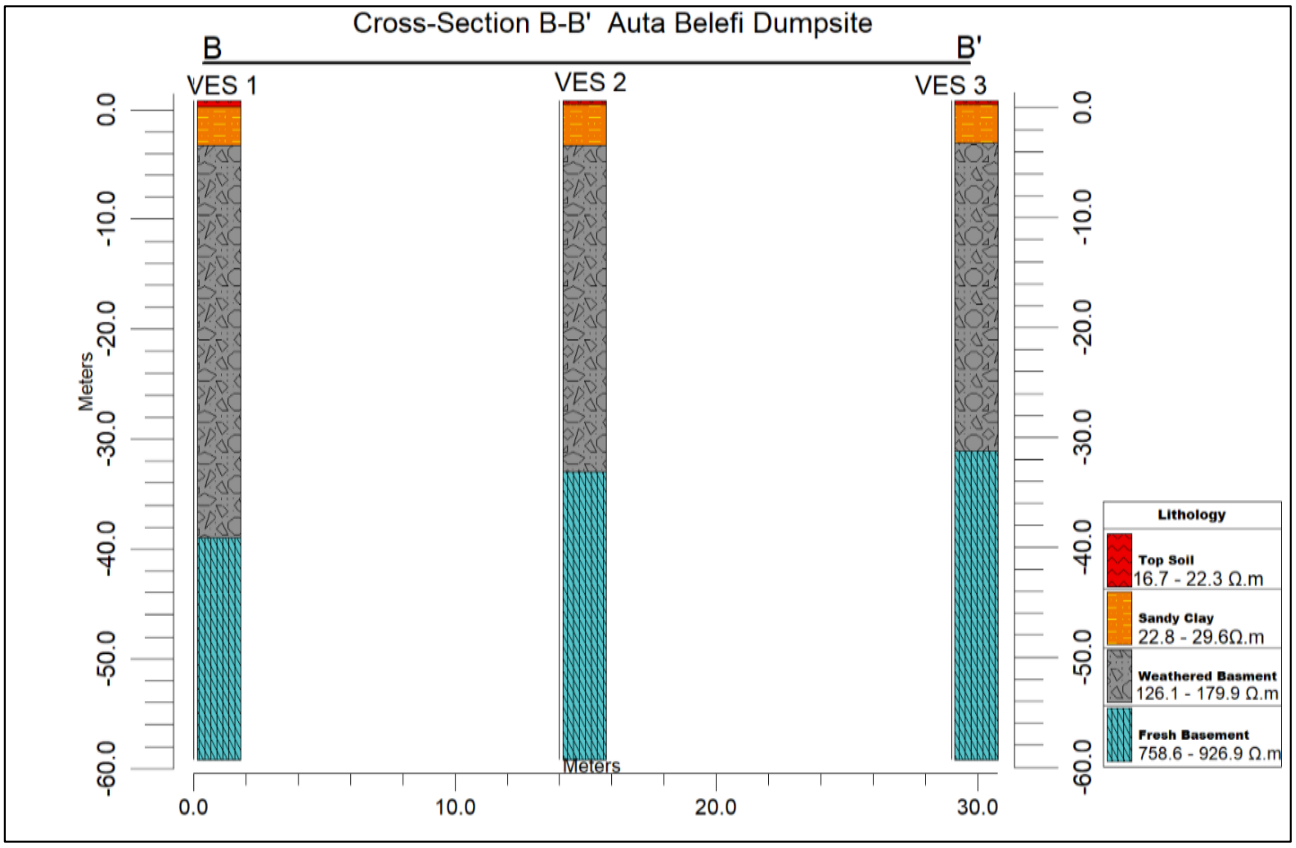

Fig 12 Hole-to-Hole Auta Balefi

ISSN No: -2456-2165 https://doi.org/10.38124/ijisrt/26apr2380

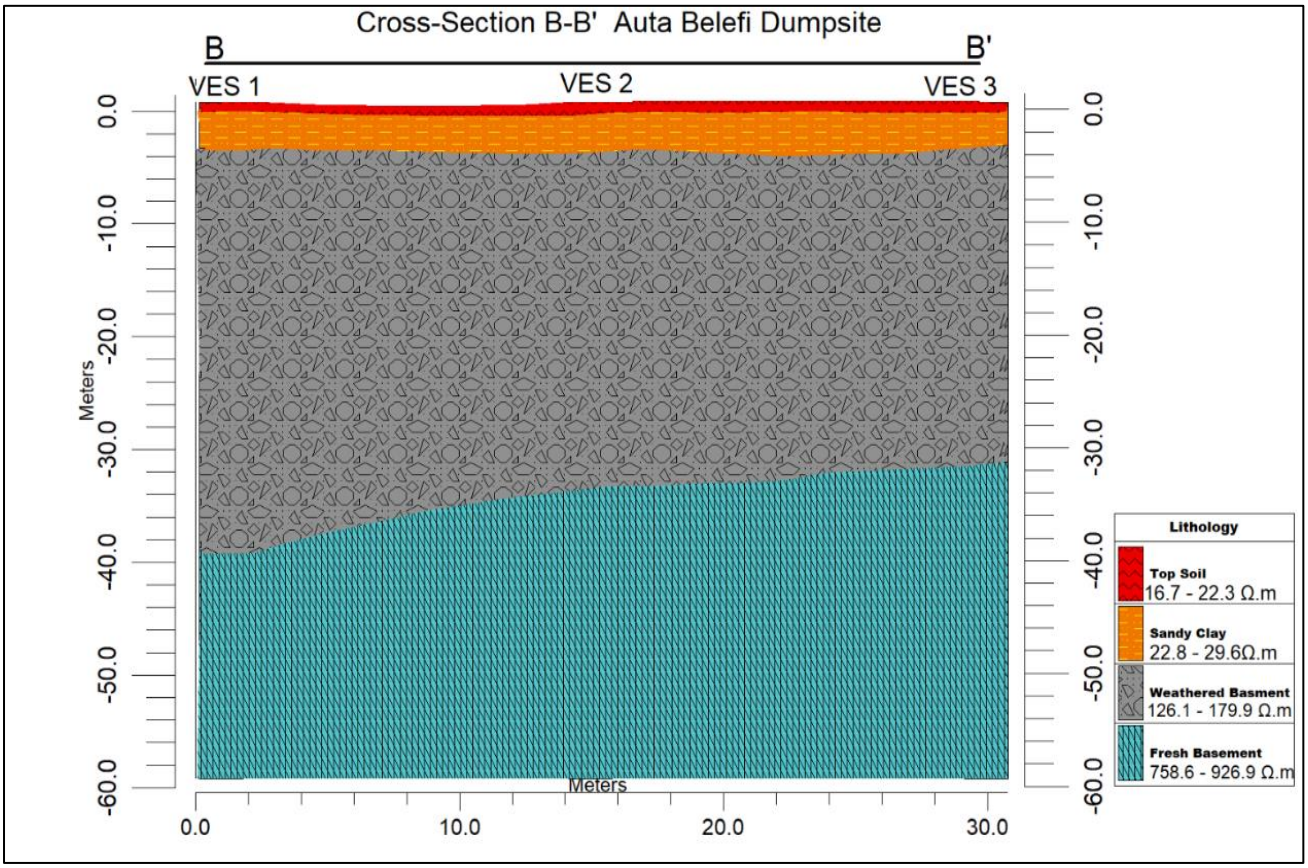

Fig 13 Geoelectric Section Auta Balefi

2D lithological model along B to B' profile (60 m depth) for Auta Balefi dumpsite, showing topsoil (0–0.6 m, 16.7–22.3 Ωm), sandy clay (0.4–4.1 m, 22.8–29.6 Ωm), weathered basement (3.9–39.8 m, 126.1–179.9 Ωm), and fresh basement (31.9–60 m, 758.6–926.9 Ωm), with low-resistivity upper layers and thickened weathered basement suggesting contamination and potential pollutant migration.

- *Tudun Wada*

The 2D lithological model and hole-to-hole section for the Tudun Wada dumpsite (C to C' profile, 40 m total depth), with VES 1 at 0 m, VES 2 at 15 m, and VES 3 at 30 m, are presented in Figures 14 (geoelectric section) and 13 (hole-to-hole section). The model identifies four lithological units: topsoil (6.2–53.8 Ωm, depth 0–1.3 m, thickness 0.4–1.3 m), sandy clay (9.1–15.8 Ωm, depth 0.4–3.8 m, thickness 1.4–3.4 m), weathered basement (81.1–554.2 Ωm, depth 2.7–12.4 m, thickness 1.9–8.7 m), and fresh basement (4150.5–11428 Ωm, depth 5.7–40 m, thickness 27.6–34.3 m). Resistivity correlations indicate highly conductive topsoil and sandy clay (5–100 Ωm) due to contamination, weathered basement (100–1000 Ωm) as altered rock, and fresh basement (>1000 Ωm) as resistive bedrock. Compared to the control point VES 4 (topsoil 117.7 Ωm, depth 0–0.8 m, thickness 0.8 m; sandy clay 53.6 Ωm, depth 0.8–5.4 m, thickness 4.6 m; weathered basement 1196.5 Ωm, depth 5.4–23.8 m, thickness 18.4 m; fresh basement 3106.6 Ωm, depth 23.8–40 m, thickness 16.2 m), dumpsite VES points show extremely low resistivity in the topsoil (6.2–7.5 Ωm at VES 2–3) and sandy clay (9.1–15.8 Ωm), with VES 2's weathered basement (81.1 Ωm) also low, indicating significant contamination.

Spatially, the topsoil thins from 1.3 m at VES 1 to 0.4 m at VES 2 and VES 3, while the weathered basement thickens from 1.9 m at VES 2 to 8.7 m at VES 3, suggesting increased weathering toward the profile's end. The low-resistivity topsoil and sandy clay layers, particularly at VES 2 and VES 3 (6.2–7.5 Ωm), form a continuous conductive zone across the 30 m profile, indicating a major pathway for lateral pollutant migration. The fresh basement's high resistivity (up to 11428 Ωm at VES 1) and thickness (27.6–34.3 m) restrict deeper migration, highlighting the need for remediation in the upper 3.8 m to prevent shallow groundwater contamination.

ISSN No: -2456-2165 https://doi.org/10.38124/ijisrt/26apr2380

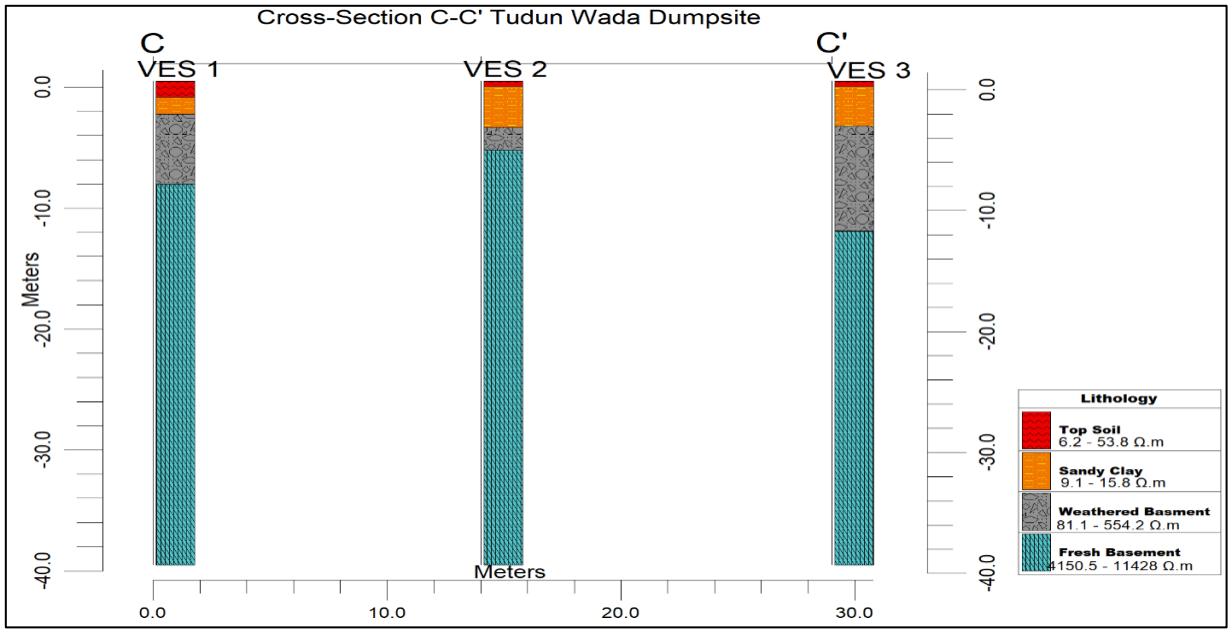

Fig 14 Hole-to-Hole

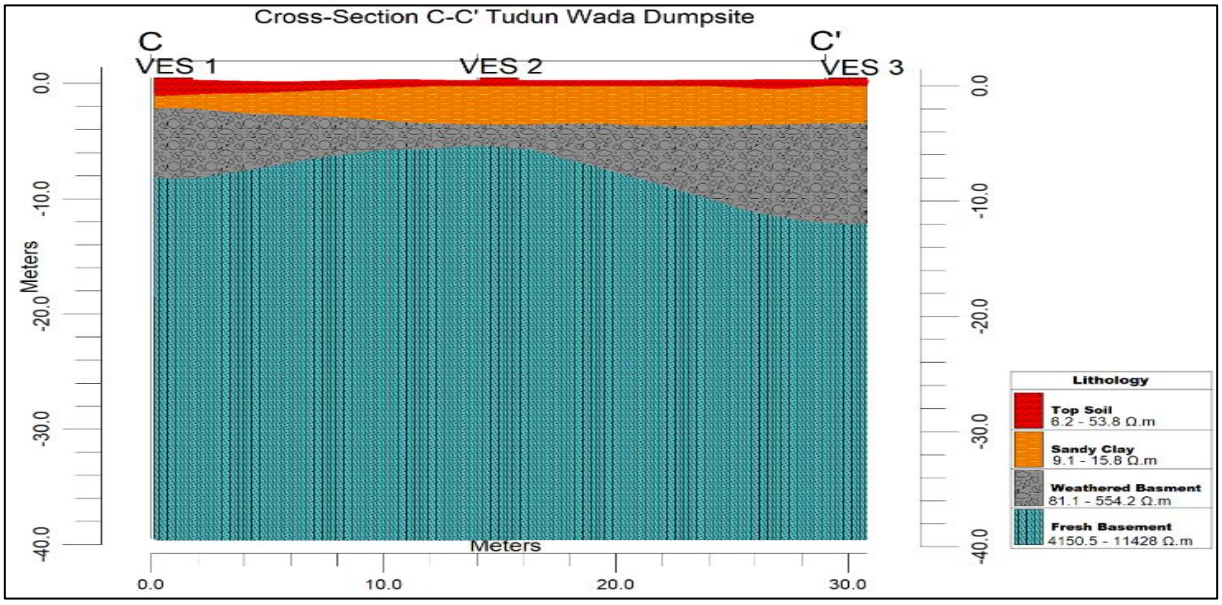

Fig 15 2D Lithological Model Along C to C' profile (40 m Depth) Tudun Wada Dumpsite

Topsoil (0–1.3 m, 6.2–53.8 Ωm), sandy clay (0.4–3.8 m, 9.1–15.8 Ωm), weathered basement (2.7–12.4 m, 81.1–554.2 Ωm), and fresh basement (5.7–40 m, 4150.5–11428 Ωm), with extremely low-resistivity topsoil at VES 2–3 indicating significant contamination and lateral pollutant migration potential.

- *Keffi*

The 2D lithological model and hole-to-hole section for the Keffi dumpsite (D to D' profile, 40 m total depth), with VES 1 at 0 m, VES 2 at 15 m, and VES 3 at 30 m, are shown in Figures 16 (geoelectric section) and 15 (hole-to-hole section). The model delineates three to four lithological units: topsoil (15.7–23.2 Ωm, depth 0–3.6 m, thickness 0.6–3.6 m), sandy clay (5.6–16.1 Ωm, depth 0.6–8 m, thickness 1.3–4.4 m), weathered basement (21.4 Ωm, depth 1.9–5 m, thickness 3.1 m at VES 2), and fresh basement (1262.8–4017.2 Ωm, depth 3.4–40 m, thickness 12.9–35 m). Resistivity correlations indicate conductive topsoil and sandy clay (5–100 Ωm) due to contamination, weathered basement (100–1000 Ωm) at VES 2, and fresh basement (>1000 Ωm) as resistive bedrock. Compared to the control point VES 4 (topsoil 195.8 Ωm, depth 0–0.6 m, thickness 0.6 m; sandy clay 93.5 Ωm, depth 0.6–4.2 m, thickness 3.6 m; clay 43.1 Ωm, depth 4.2–8.6 m, thickness 4.4 m; fresh basement 5783 Ωm, depth 8.6–40 m, thickness 31.4 m), dumpsite VES points show significantly lower resistivity in the topsoil (15.7–23.2 Ωm) and sandy clay (5.6–16.1 Ωm), with VES 2's weathered basement (21.4 Ωm) indicating deep contamination.

Spatially, the topsoil thickens from 0.6 m at VES 2 to 3.6 m at VES 3, while the sandy clay layer varies from 1.3 m at VES 2 to 4.4 m at VES 3. The extremely low resistivity

ISSN No: -2456-2165 https://doi.org/10.38124/ijisrt/26apr2380

in the sandy clay at VES 1 (5.6 Ωm) and VES 2 (11.4 Ωm) forms a continuous conductive zone, suggesting a primary pathway for lateral pollutant migration, particularly at the profile's start. The fresh basement's high resistivity (up to 4017.2 Ωm) and thickness (12.9–35 m) limit deeper migration, emphasizing the need for remediation in the upper 8 m to protect shallow groundwater.

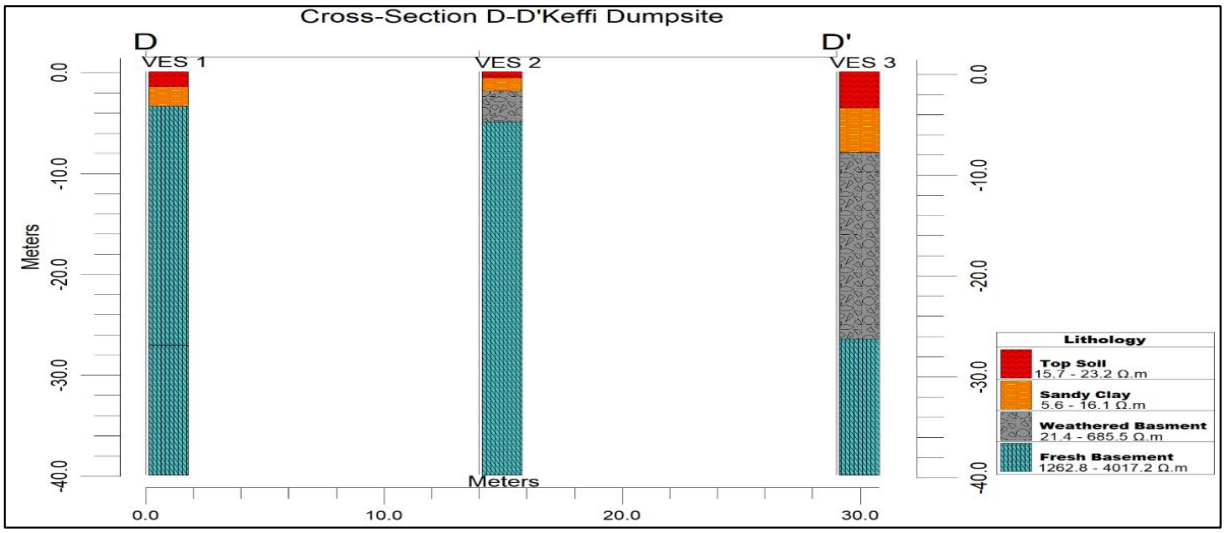

Fig 16 Hole-to-Hole

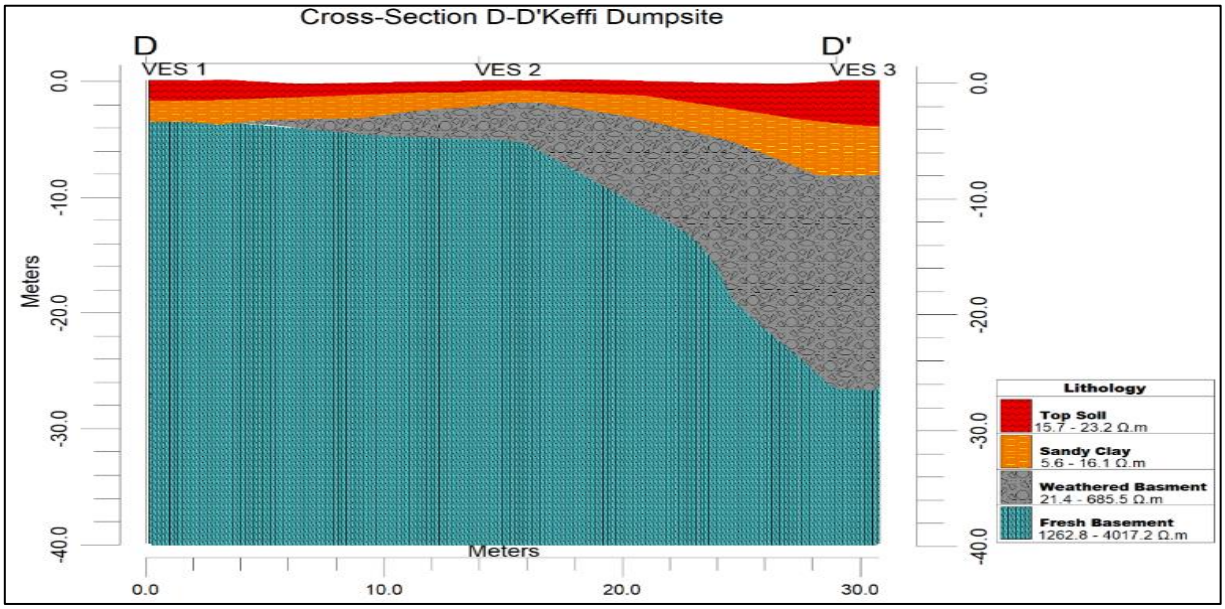

Figure 17 2D Lithological Model Along D to D' Profile (40 m Depth) Keffi Dumpsite

Topsoil (0–3.6 m, 15.7–23.2 Ωm), sandy clay (0.6–8 m, 5.6–16.1 Ωm), weathered basement (1.9–5 m, 21.4 Ωm at VES 2), and fresh basement (3.4–40 m, 1262.8–4017.2 Ωm), with very low-resistivity sandy clay indicating significant contamination and lateral pollutant migration.

- *Pseudo-Sections for Subsurface Apparent Resistivity Distribution and Contamination Assessment*

Pseudo-sections offer a pseudo-2D visualization of subsurface apparent resistivity distribution, constructed by interpolating data from vertical electrical sounding (VES) points across a profile. For the four dumpsite locations; Angwa Adamu Kugbaru Ado, Auta Balefi, Tudun Wada and Keffi pseudo-sections were generated to complement the 2D lithological models and hole-to-hole sections. These pseudo-sections, plotted as colourful maps with blue representing low apparent resistivity (5–100 Ωm, indicative of conductive zones potentially associated with contamination) and pink representing high apparent resistivity (>1000 Ωm, indicative of resistive bedrock), provide a continuous view of lateral and vertical resistivity variations across the VES profiles (0–30 m, with VES 1 at 0 m, VES 2 at 15 m, and VES 3 at 30 m). The pseudo-sections extend to depths of 50 m for Angwa Adamu Kugbaru Ado, 60 m for Auta Balefi and 40 m for Tudun Wada and Keffi, consistent with the lithological models. By focusing on apparent resistivity values, these sections highlight anomalies such as conductive zones likely caused by leachate infiltration, offering insights into contamination patterns and complementing the lithological models by providing a

ISSN No: -2456-2165 https://doi.org/10.38124/ijisrt/26apr2380

broader perspective on subsurface resistivity distribution. The sections also contrast dumpsite data with control point VES 4 to emphasize contamination-related anomalies.

- *Angwa Adamu Kugbaru Ado*

The pseudo-section for Angwa Adamu Kugbaru Ado (A to A' profile, 50 m depth), shown in Figure 4.29, is constructed from VES 1 (0 m), VES 2 (15 m), and VES 3 (30 m). It displays apparent resistivity variations corresponding to lithological units: topsoil (56.7–68.7 Ωm, depth 0–1.2 m, blue), sandy clay (22.8–28.6 Ωm, depth 1–5.7 m, blue), weathered basement (348.2–895.2 Ωm, depth 4.3–14.9 m, green to yellow), and fresh basement (10504–11811.7 Ωm, depth 9.7–50 m, pink). The low apparent resistivity in the topsoil and sandy clay layers (blue zones, 22.8–68.7 Ωm) across the 30 m profile, particularly at VES 3 (56.7 Ωm topsoil, 25.5 Ωm sandy clay), indicates conductive anomalies suggestive of leachate contamination. Compared to the control point VES 4 (topsoil 103.5 Ωm, depth 0–1 m; sandy clay 32.7 Ωm, depth 1–4.2 m; weathered basement 617.3 Ωm, depth 4.2–15.1 m; fresh basement 9105.1 Ωm, depth 15.1–50 m), the dumpsite's upper layers show significantly lower resistivity, confirming pollution. The blue zone's lateral continuity in the sandy clay layer (22.8–28.6 Ωm, up to 5.7 m depth) suggests a pathway for pollutant migration, potentially affecting shallow groundwater. The pink fresh basement (10504–11811.7 Ωm, up to 50 m depth) acts as a resistive barrier, limiting deeper migration. The pseudo-section enhances the lithological model (Figures 4.15–4.16) by visualizing the extensive low-resistivity zone, emphasizing the contamination's spatial extent in the upper 5.7 m.

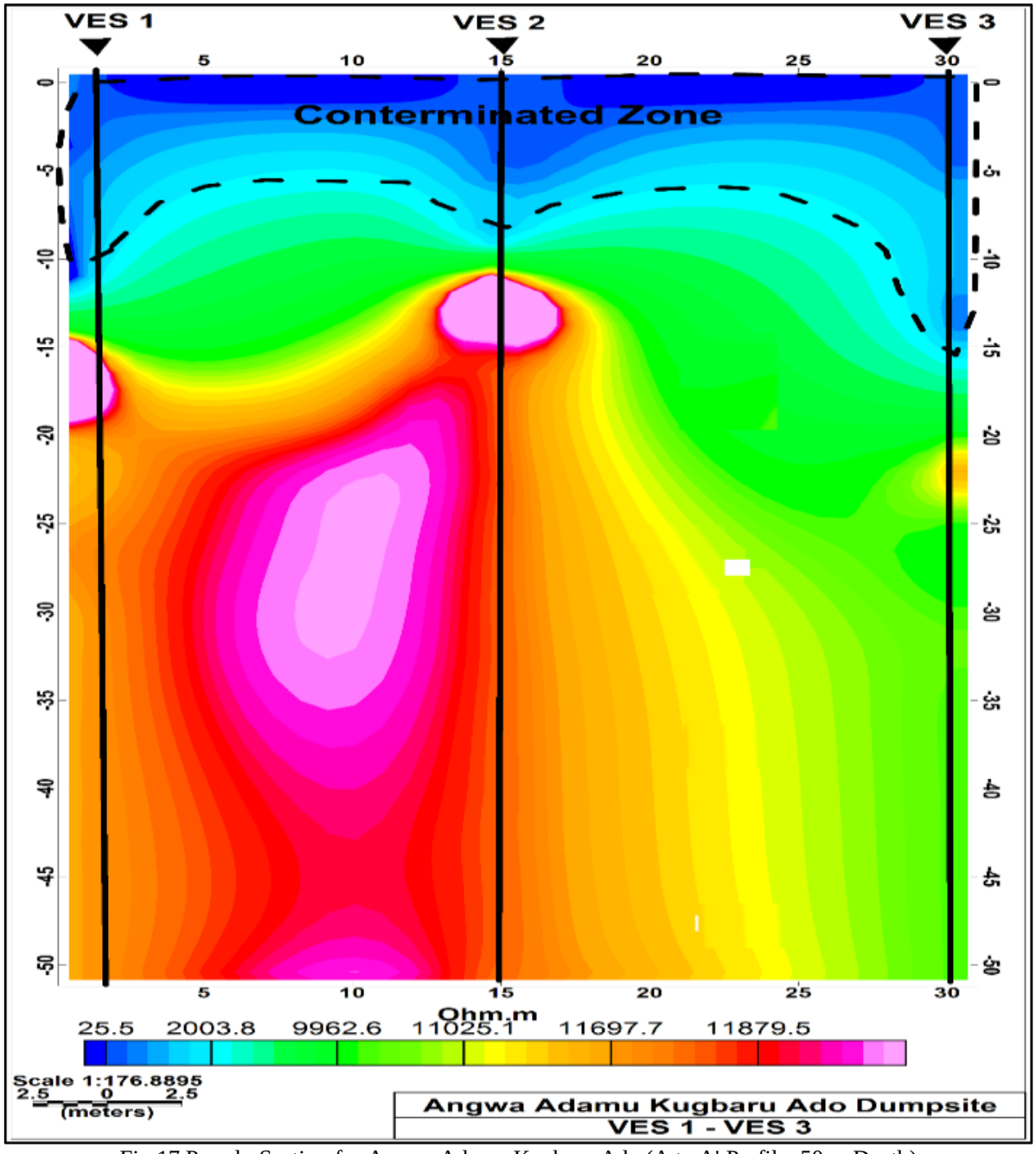

Fig 17 Pseudo-Section for Angwa Adamu Kugbaru Ado (A to A' Profile, 50 m Depth)

ISSN No: -2456-2165 https://doi.org/10.38124/ijisrt/26apr2380

The blue colour indicates low-resistivity zones (56.7–68.7 Ωm topsoil, 0–1.2 m; 22.8–28.6 Ωm sandy clay, 1–5.7 m) indicating leachate contamination, green to yellow weathered basement (348.2–895.2 Ωm, 4.3–14.9 m), and pink fresh basement (10504–11811.7 Ωm, 9.7–50 m) as a resistive barrier across the 30 m profile.

- *Auta Balefi*

The pseudo-section for Auta Balefi (B to B' profile, 60 m depth), shown in Figure 4.30, is derived from VES 1 (0 m), VES 2 (15 m), and VES 3 (30 m). It displays apparent resistivity variations: topsoil (16.7–22.3 Ωm, depth 0–0.6 m, blue), sandy clay (22.8–29.6 Ωm, depth 0.4–4.1 m, blue), weathered basement (126.1–179.9 Ωm, depth 3.9–39.8 m, green), and fresh basement (758.6–926.9 Ωm, depth 31.9–60 m, pink). The low apparent resistivity in the topsoil (16.7–22.3 Ωm) and sandy clay (22.8–29.6 Ωm), particularly at VES 2 (16.7 Ωm topsoil, 22.8 Ωm sandy clay), forms prominent blue zones indicative of conductive anomalies, likely due to leachate infiltration. Compared to the control point VES 4 (topsoil 139.7 Ωm, depth 0–1.7 m; sandy clay 53.8 Ωm, depth 1.7–2.9 m; weathered basement 107.8 Ωm, depth 2.9–49.9 m; fresh basement 909 Ωm, depth 49.9–60 m), the dumpsite's low resistivity in the upper layers (0–4.1 m) and weathered basement (126.1–179.9 Ωm) suggests pollutant infiltration. The blue zones extend laterally across the 30 m profile, forming a continuous conductive zone that facilitates lateral pollutant migration, particularly pronounced at 15 m (VES 2). The pink fresh basement (758.6–926.9 Ωm) limits deeper migration. The pseudo-section complements the lithological model (Figures 4.17–4.18) by highlighting the spatial extent of the conductive zone in the upper 4.1 m, critical for assessing shallow groundwater contamination risks.

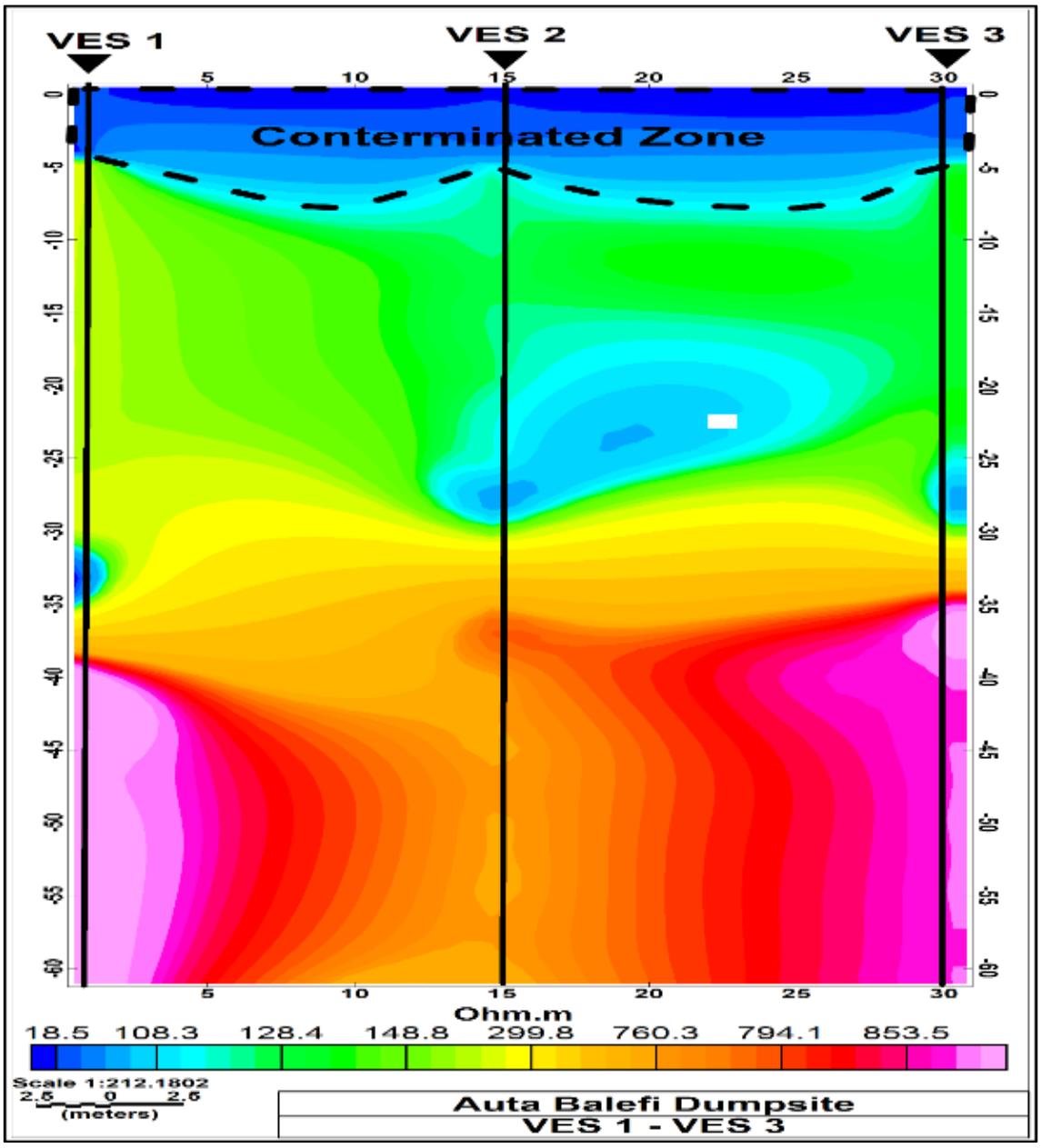

Fig 18 Pseudo-Section for Auta Balefi (B to B' Profile, 60 m Depth)

ISSN No: -2456-2165 https://doi.org/10.38124/ijisrt/26apr2380

The blue colour indicates a low-resistivity zones (16.7–22.3 Ωm topsoil, 0–0.6 m; 22.8–29.6 Ωm sandy clay, 0.4–4.1 m) indicating leachate contamination, green weathered basement (126.1–179.9 Ωm, 3.9–39.8 m), and pink fresh basement (758.6–926.9 Ωm, 31.9–60 m) as a resistive barrier across the 30 m profile.

- *Tudun Wada*

The pseudo-section for Tudun Wada (C to C' profile, 40 m depth), shown in Figure 4.31, is constructed from VES 1 (0 m), VES 2 (15 m), and VES 3 (30 m). It displays apparent resistivity variations: topsoil (6.2–53.8 Ωm, depth 0–1.3 m, blue), sandy clay (9.1–15.8 Ωm, depth 0.4–3.8 m, blue), weathered basement (81.1–554.2 Ωm, depth 2.7–12.4 m, green to yellow), and fresh basement (4150.5–11428 Ωm, depth 5.7–40 m, pink). The intensely low apparent resistivity in the topsoil (6.2–7.5 Ωm at VES 2–3) and sandy clay (9.1 Ωm at VES 1, 11.8 Ωm at VES 3) forms prominent blue zones, indicating significant conductive anomalies likely due to leachate contamination. Compared to the control point VES 4 (topsoil 117.7 Ωm, depth 0–0.8 m; sandy clay 53.6 Ωm, depth 0.8–5.4 m; weathered basement 1196.5 Ωm, depth 5.4–23.8 m; fresh basement 3106.6 Ωm, depth 23.8–40 m), the dumpsite's upper layers (0–3.8 m) and weathered basement at VES 2 (81.1 Ωm) show markedly lower resistivity, suggesting deep pollutant influence. The blue zones extend across the 30 m profile, indicating a major pathway for lateral pollutant migration, particularly at 15–30 m (VES 2–3). The pink fresh basement (up to 11428 Ωm) restricts deeper migration. The pseudo-section enhances the lithological model (Figures 4.19–4.20) by visualizing the extensive conductive zone in the upper 3.8 m, critical for remediation planning.

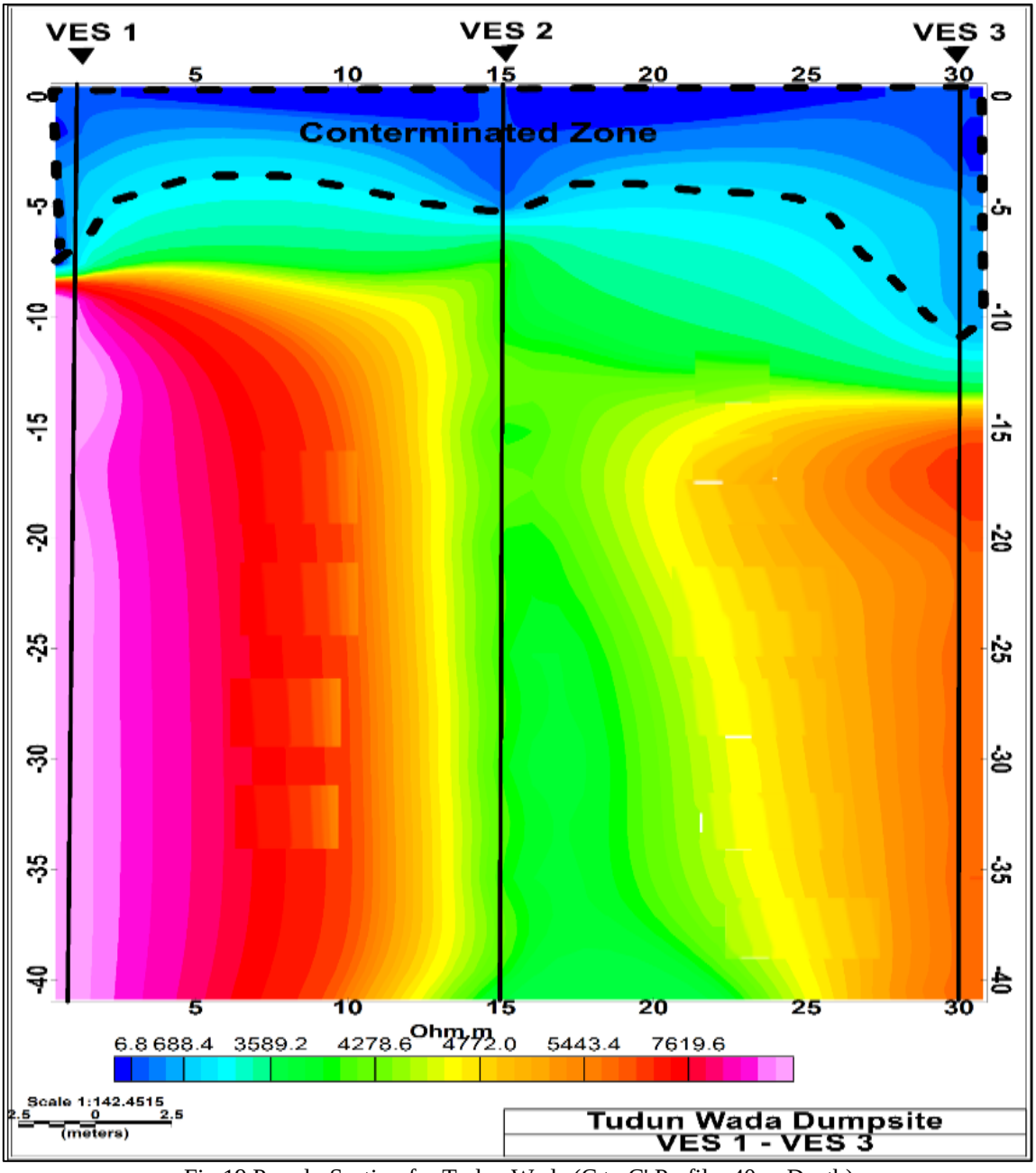

Fig 19 Pseudo-Section for Tudun Wada (C to C' Profile, 40 m Depth)

ISSN No: -2456-2165 https://doi.org/10.38124/ijisrt/26apr2380

The intense blue colour is showing a low-resistivity zones (6.2–53.8 Ωm topsoil, 0–1.3 m; 9.1–15.8 Ωm sandy clay, 0.4–3.8 m) indicating significant leachate contamination, green to yellow weathered basement (81.1–554.2 Ωm, 2.7–12.4 m), and pink fresh basement (4150.5–11428 Ωm, 5.7–40 m) across the 30 m profile.

- *Keffi*

The pseudo-section for Keffi (D to D' profile, 40 m depth), shown in Figure 4.32, is derived from VES 1 (0 m), VES 2 (15 m), and VES 3 (30 m). It displays apparent resistivity variations: topsoil (15.7–23.2 Ωm, depth 0–3.6 m, blue), sandy clay (5.6–16.1 Ωm, depth 0.6–8 m, blue), weathered basement (21.4 Ωm, depth 1.9–5 m at VES 2, blue-green), and fresh basement (1262.8–4017.2 Ωm, depth 3.4–40 m, pink). The extremely low apparent resistivity in the sandy clay at VES 1 (5.6 Ωm) and VES 2 (11.4 Ωm), along with the topsoil (15.7–23.2 Ωm), forms intense blue zones indicative of conductive anomalies, strongly suggestive of leachate contamination. The weathered basement at VES 2 (21.4 Ωm, blue-green) further indicates deep pollutant infiltration. Compared to the control point VES 4 (topsoil 195.8 Ωm, depth 0–0.6 m; sandy clay 93.5 Ωm, depth 0.6–4.2 m; clay 43.1 Ωm, depth 4.2–8.6 m; fresh basement 5783 Ωm, depth 8.6–40 m), the dumpsite's upper layers (0–8 m) show significantly lower resistivity. The blue zones extend across the 30 m profile, suggesting a continuous pathway for lateral pollutant migration, particularly pronounced at 0–15 m (VES 1–2). The pink fresh basement (up to 4017.2 Ωm) limits deeper migration. The pseudo-section enhances the lithological model (Figures 4.21–4.22) by highlighting the severe conductive anomaly in the upper 8 m, critical for assessing contamination risks.

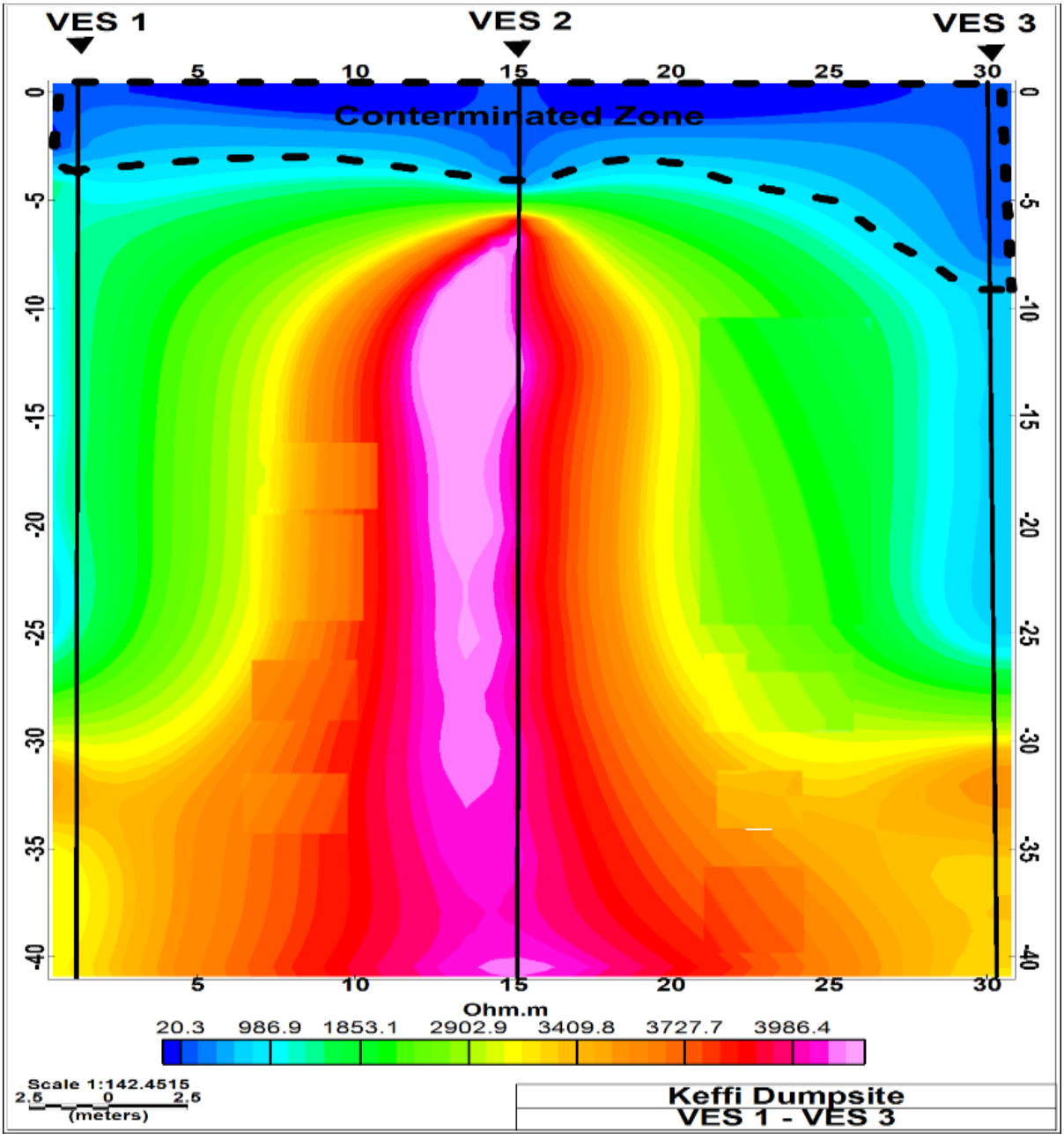

Fig 20 Pseudo-Section for Keffi (D to D' Profile, 40 m Depth)

ISSN No: -2456-2165 https://doi.org/10.38124/ijisrt/26apr2380

An intense blue low-resistivity zones (15.7–23.2 Ωm topsoil, 0–3.6 m; 5.6–16.1 Ωm sandy clay, 0.6–8 m) indicating severe leachate contamination, blue-green weathered basement (21.4 Ωm, 1.9–5 m at VES 2), and pink fresh basement (1262.8–4017.2 Ωm, 3.4–40 m) across the 30 m profile.

➢ *Results of Water Analysis*

- *Interpretation of Water Sample Analysis at Angwa Adamu Kugbaru Ado*

✓ *Heavy Metals (Cr, Ni, Mn, Cu, Cd, Co, Pb, Fe, Zn)*

The concentrations of heavy metals across the sampled locations show clear spatial variations that reflect differing degrees of contamination. Chromium (Cr) levels are highest in Control 1 (0.482 mg/L), moderately high at the dump site (0.210 mg/L), and lowest in Control 2 (0.134 mg/L). Although Control 1 unexpectedly records the highest Cr concentration, the dump site still exhibits elevated values relative to Control 2, suggesting leachate influence. Nickel (Ni), Manganese (Mn), and Zinc (Zn) follow a similar trend, where Control 2 records higher values for Ni (0.098 mg/L) and Mn (0.256 mg/L) compared to the dump site, indicating potential anthropogenic inputs unrelated to dumpsite activity. However, the dump site still shows elevated Zn and Mn values compared to Control 1.

Lead (Pb) and Iron (Fe) concentrations are particularly notable. Control 1 exhibits the highest Pb (1.196 mg/L) and Fe (1.695 mg/L), values far exceeding WHO permissible limits (0.01 mg/L for Pb and 0.3 mg/L for Fe). The dump site also shows high Pb (0.799 mg/L) and Fe (0.452 mg/L), confirming contamination likely linked to waste decomposition and metal leaching. Copper (Cu) and Cadmium (Cd) values at the dump site remain relatively low compared to the controls, but Cu at the dump site (0.261 mg/L) is still significantly above WHO limits (0.05 mg/L), presenting potential health risks.

✓ *Major Cations (Ca, Mg, Na, K)*

Calcium (Ca) and Magnesium (Mg) values indicate moderate hardness levels in all locations, with the dump site showing elevated Ca (13.53 mg/L) and Mg (8.14 mg/L). The high Ca and Mg values at both the dump site and Control 1 suggest mineral-rich geology or possible leachate influence. Sodium (Na) concentrations are highest at the dump site (12.70 mg/L), implying infiltration of saline or ionic constituents from waste materials. Potassium (K) shows a moderate distribution with slightly elevated values in Control 2 (7.57 mg/L), although the dump site's concentration (6.16 mg/L) also reflects potential pollutant loading. Overall, the elevated cation levels at the dump site suggest enhanced ionic dissolution from waste degradation.

✓ *Turbidity and Conductivity*

Turbidity values across the sampling points are low, with the dump site recording the lowest turbidity (0.47 NTU), suggesting minimal suspended solids visually. However, this does not necessarily indicate low contamination, as dissolved pollutants do not influence turbidity. Conductivity, which reflects the total dissolved ionic content, is highest at the dump site (551.8 µS/cm), strongly indicating higher levels of dissolved inorganic matter likely originating from waste leachates. Control 1 also shows elevated conductivity (459.7 µS/cm), while Control 2 (241.5 µS/cm) remains comparatively lower, suggesting less contamination or mineral dissolution.

✓ *pH and Dissolved Oxygen (DO)*

The pH levels across the samples are slightly acidic, with Control 2 showing the lowest pH (5.14), followed by the dump site (5.82) and Control 1 (6.43). The acidity at the dump site may be attributed to organic waste decomposition, which releases acids into the groundwater. Dissolved Oxygen (DO) values are highest at the dump site (10.4 mg/L), contrary to typical expectations of oxygen depletion near polluted sites. This anomaly may indicate shallow sampling, fast-moving water, or recent aeration. Control 2 shows moderately high DO (9.45 mg/L), while Control 1 registers slightly lower values (8.56 mg/L). Overall, the DO levels indicate adequate oxygenation but do not negate chemical contamination.

✓ *Suspended Solids and Nutrient Levels (TSS, Phosphate, Sulphate, Nitrate)*

Total Suspended Solids (TSS) show a strong gradient from Control 1 (2.25 mg/L) to Control 2 (5.04 mg/L) and sharply rising at the dump site (15.35 mg/L). This suggests particulate pollution originating from the dumpsite's leachate and soil disturbance. Nutrient levels also show significant variation. Phosphate concentrations are highest at the dump site (1.18 mg/L), indicating organic waste influence. Sulphate levels remain very low across all sites, but the dump site (0.04 mg/L) still shows a slight elevation compared to Control 2.

Nitrate levels exhibit the most striking difference. The dump site shows an exceptionally high concentration (28.45 mg/L) compared to both controls (0.45 and 0.64 mg/L). This sharp elevation confirms heavy contamination from decomposing organic waste, sewage infiltration, or fertilizer-rich refuse. Elevated nitrate levels pose serious health risks such as methemoglobinemia ("blue baby syndrome") and environmental risks such as eutrophication.

✓ *Hardness*

Water hardness, primarily influenced by Ca and Mg concentrations, follows the pattern: Dump Site (10 mg/L) > Control 1 (6 mg/L) > Control 2 (3.8 mg/L). The increased hardness at the dump site corresponds to the elevated cation concentrations, indicating mineral dissolution from waste leachate interacting with subsurface materials.

✓ *Summary of the Interpretation*

The overall analysis indicates that the dump site exhibits higher levels of contamination relative to both control sites, especially in conductivity, TSS, nitrate, chloride, and several heavy metals. Although some parameters such as Cr, Pb, and Fe were unexpectedly higher

ISSN No: -2456-2165 https://doi.org/10.38124/ijisrt/26apr2380

in Control 1, the dump site still shows strong signatures of leachate influence. The elevated nitrate, chloride, conductivity, and suspended solids at the dump site confirm waste-derived pollution. These results collectively suggest that the groundwater or surface water near the dump site is significantly impacted by anthropogenic activities, posing potential environmental and public health risks.

- *Analysis and Interpretation of Water Sample Results – Auta Balefi*

The physicochemical and heavy metal analyses of water samples collected from Auta Balefi reveal significant variations between the control sites and the dump-site sample (Table 4.2). The results suggest clear evidence of contamination at the dump site, likely driven by leachate infiltration and pollutant transport from surrounding waste deposition. The parameters analyzed provide insight into the water quality status and the potential public health risks associated with exposure.

✓ *Chromium (Cr)*

Chromium concentrations at the dump site (0.82 mg/L) are markedly higher than at Control 1 (0.48 mg/L) and Control 2 (0.13 mg/L). This value exceeds WHO's permissible limit of 0.05 mg/L. The elevated level indicates strong contamination from industrial or metallic waste within the dump site. Chromium is toxic and carcinogenic, posing risks of kidney damage and gastrointestinal distress.

✓ *Potassium (K)*

Potassium levels are significantly elevated at the dump site (10.12 mg/L) compared to both controls (5.68–7.57 mg/L). This suggests leaching from decomposing organic waste, ash, and fertilizer remnants. Though potassium is not highly toxic, persistently elevated concentrations indicate nutrient loading and chemical inputs.

✓ *Calcium (Ca)*

Calcium values at the dump site (12 mg/L) remain lower than Control 1 (16.49 mg/L) but higher than Control 2 (3.20 mg/L). This suggests moderate Ca enrichment likely due to cement, construction waste, and carbonate-bearing materials within the dump. The level does not pose a direct health concern but reflects mineral alteration of infiltrating water.

✓ *Nickel (Ni)*

Nickel concentration is extremely elevated at the dump site (0.99 mg/L) relative to both controls (<0.1 mg/L). This is far above the WHO limit of 0.02 mg/L, indicating severe contamination. Ni exposure can cause dermatitis, respiratory problems, and organ toxicity, pointing to metallic disposals (batteries, alloys) as pollution sources.

✓ *Magnesium (Mg)*

Magnesium levels (6.5 mg/L) at the dump site closely mirror natural background concentrations from the controls but remain slightly elevated. This suggests minor influence from mineral dissolution rather than significant contamination.

✓ *Manganese (Mn)*

The dump site shows a high Mn concentration (1.13 mg/L), greatly exceeding both controls and surpassing the WHO limit of 0.4 mg/L. Manganese-rich contamination is typically associated with battery waste, welding residues, and metal scraps. High Mn causes neurological disorders with long-term exposure.

✓ *Sodium (Na)*

Sodium concentrations at the dump site (10 mg/L) are within normal background levels and resemble the control sites. This indicates limited influence from saline leachates or salt-containing wastes.

✓ *Copper (Cu)*

Copper shows a dramatic increase at the dump site (28.78 mg/L) compared to near-zero levels in the controls. This far exceeds WHO limits (2 mg/L) and indicates major contamination from electrical wires, metal scraps, pesticides, and plumbing materials. High copper levels can cause gastrointestinal irritation and liver damage.

✓ *Cadmium (Cd)*

Cadmium levels jump to 0.89 mg/L at the dump site, compared to very low levels in controls (≤0.026 mg/L). This is profoundly above the WHO limit of 0.003 mg/L. Cadmium contamination is indicative of battery disposal, plastics, pigments, and electronic waste. Chronic exposure leads to kidney damage and bone demineralization.

✓ *Cobalt (Co)*

Cobalt levels are elevated at the dump site (1.26 mg/L), greatly exceeding control values. This suggests leaching from rechargeable batteries, alloys, and paints. Such levels are harmful, affecting the cardiovascular and hematological systems.

✓ *Lead (Pb)*

Lead levels (1.41 mg/L) at the dump site are higher than at both controls, with all values exceeding the WHO limit (0.01 mg/L). Lead contamination likely arises from batteries, solder, paints, and pipes. Lead is a potent neurotoxin, especially harmful to children.

✓ *Iron (Fe)*

Iron levels are moderate at 0.53 mg/L at the dump site, lower than Control 1 but slightly higher than Control 2. This suggests limited but notable iron input from corroded metals in waste. Levels above 0.3 mg/L affect taste and may cause discoloration.

✓ *Zinc (Zn)*

Zinc at the dump site (0.5 mg/L) is significantly higher than both controls. This indicates contamination from galvanized materials, batteries, and metal coatings. Although zinc is essential, excess levels can cause nausea and vomiting.

✓ *Turbidity*

Turbidity at the dump site is moderate (0.55 NTU) and lower than controls. This suggests that although

ISSN No: -2456-2165 https://doi.org/10.38124/ijisrt/26apr2380

contaminants are high, they are largely dissolved rather than particulate, indicating efficient leachate infiltration into groundwater.

✓ *Electrical Conductivity (EC)*

Electrical conductivity is significantly elevated at the dump site (881 µS/cm), nearly double Control 1 and triple Control 2. This indicates high ionic loading due to dissolved salts and metals from waste leachate infiltration into groundwater.

✓ *pH*

The dump site water has a near-neutral to slightly alkaline pH of 7.83, contrasting with the acidic control sites. The shift toward alkalinity indicates buffering by cement, ash, and metallic waste. This pH facilitates the mobility of heavy metals.

✓ *Total Suspended Solids (TSS)*

TSS is elevated at the dump site (9 mg/L), higher than both controls. Increased TSS reflects suspended organic and inorganic particles from surface runoff and decomposing waste.

✓ *Dissolved Oxygen (DO)*

DO is slightly elevated at the dump site (10 mg/L), likely from photosynthetic activity or aeration during sampling. However, this may mask underlying microbial oxygen demand from waste breakdown.

✓ *Chloride*

Chloride levels (176 mg/L) are extremely high compared to controls (<26 mg/L). This indicates strong contamination from leachates, sewage components, and household waste. High chloride accelerates metal corrosion and can affect taste.

✓ *Phosphate*

Phosphate concentration at the dump site (6.36 mg/L) is drastically higher than controls, signaling contamination from detergents, food waste, fertilizers, and organic materials. This promotes eutrophication.

✓ *Sulphate*

Sulphate levels remain low across all samples, suggesting minimal influence from sulphate-rich waste materials.

✓ *Nitrate*

Nitrate levels (38 mg/L) are significantly elevated compared to the controls (<1 mg/L). The value exceeds WHO limits (10 mg/L for infants), indicating contamination from organic waste, sewage, and fertilizers. High nitrate can cause methemoglobinemia (“blue baby syndrome”).

✓ *Hardness*

Hardness remains similar across samples, indicating limited influence from waste disposal. Slight elevation at the dump site suggests additional contributions from Ca–Mg minerals.

✓ *Summary of The Interpretation*

The dump-site water sample shows significant contamination, especially in heavy metals (Cr, Ni, Mn, Cu, Cd, Co, Pb), nutrients (phosphate, nitrate), chloride, and conductivity. These results demonstrate active leachate infiltration and pollutant transport from the waste dump into the surrounding groundwater system.

Key indicators of contamination:

- Extremely high heavy metals (Cu, Cd, Pb, Ni)
- High nutrient pollution (nitrate, phosphate)
- High EC and chloride
- pH shift suggesting chemical leachate interaction

Environmental and Public Health Implication

Such water is not safe for drinking, domestic use, or irrigation. It poses:

- Carcinogenic risks
- Neurological damage
- Kidney failure
- Gastrointestinal harm
- Ecological disturbances

Immediate mitigation, groundwater protection, and community awareness are strongly recommended.

- *Analysis And Interpretation Of Water Sample Results (Tudun Wada)*

The analysis of water samples from Tudun Wada (Table 4.3) including two control points (Control 1 and Control 2) and a dump-site location, reveals clear variations in physicochemical and heavy-metal concentrations, indicating the influence of pollutant transport from the waste-disposal area. The results provide insights into potential contamination pathways and the overall water quality status of the area.

✓ *Heavy Metals (Cr, Ni, Cd, Co, Pb, Cu, Mn, Fe, Zn)*

Chromium (Cr) concentrations ranged from 0.134 mg/L at Control 2 to 0.276 mg/L at the dump site. The elevated level at the dump site indicates possible leaching of chromium-bearing wastes into the groundwater. Although Control 1 also shows relatively high chromium, the increase at the dump site suggests localized contamination. Similarly, Nickel (Ni), Cadmium (Cd), Cobalt (Co), and Zinc (Zn) show higher concentrations at the dump site compared to at least one control point, which aligns with typical pollutant migration patterns from waste disposal sites. Of particular concern is Lead (Pb), which shows a high concentration at Control 1 (1.196 mg/L) but remains significantly high at the dump site (0.906 mg/L). These values far exceed the WHO permissible limit of 0.01 mg/L, indicating severe contamination that may pose long-term health risks such as neurological and renal damage.

Iron (Fe) levels show a significant drop from Control 1 (1.695 mg/L) to the dump site (0.880 mg/L), suggesting possible geochemical variations or adsorption processes.

ISSN No: -2456-2165 https://doi.org/10.38124/ijisrt/26apr2380

Copper (Cu) shows a relatively low level at the dump site (0.022 mg/L), indicating that copper is not a major contributor to contamination in this area. Manganese (Mn) and Zinc (Zn) also exhibit slight elevations at the dump site, although within moderate concentration levels. Overall, the heavy-metal profile suggests anthropogenic contamination with potential leachates migrating toward groundwater sources.

✓ *Major Cations (Ca, Mg, Na, K)*

Calcium (Ca) concentrations were notably high at Control 1 (16.49 mg/L) and the dump site (14.34 mg/L) but low at Control 2 (3.20 mg/L). This pattern suggests that aquifer geology, particularly the presence of limestone or related minerals, contributes more significantly to Ca levels than waste leachates. Magnesium (Mg) levels also show a similar trend, with higher concentrations at both Control 1 and the dump site, likely due to natural geologic dissolution. Sodium (Na) and Potassium (K) values are generally comparable across the locations, but slightly elevated Na at the dump site (11.46 mg/L) could indicate early signs of leachate infiltration. Potassium levels remain fairly stable, suggesting minimal influence from anthropogenic waste sources.

✓ *Physical Parameters (Turbidity, Conductivity, pH, TSS, DO)*

Turbidity shows a slight increase at the dump site (1.08 NTU) relative to Control 2 (0.8 NTU), implying mild particulate contamination, although still within acceptable limits. Electrical conductivity (EC) is notably higher at the dump site (417.7 µS/cm) compared to Control 2 (241.5 µS/cm), indicating the presence of dissolved ions often associated with waste leachates. pH values show acidic tendencies at Control 2 (5.14), while the dump site registers mildly acidic conditions (5.79), reflecting weakly acidic leachate percolation but still within a range that can influence metal solubility and enhance mobility.

Total Suspended Solids (TSS) show a significant increase at the dump site (12 mg/L), reflecting particulate matter introduced by waste degradation processes. Dissolved Oxygen (DO) levels show slightly higher values at the dump site (9.47 mg/L), possibly due to increased algal activity or aeration, but may also reflect sampling variability. Overall, the physical parameters indicate moderate alterations in water quality attributable to the proximity of waste disposal.

✓ *Anions (Chloride, Phosphate, Sulphate, Nitrate)*

Chloride concentrations are markedly higher at the dump site (31.84 mg/L) compared to the controls, signifying wastewater influence since chloride is a common indicator of anthropogenic pollution. Phosphate values also increase at the dump site (0.953 mg/L), likely associated with detergents, organic refuse, or food waste. Sulphate levels remain low and stable across all locations, indicating minimal sulphate contamination. In contrast, Nitrate shows a dramatic increase at the dump site (18 mg/L) relative to controls (0.45–0.64 mg/L). This substantial rise strongly indicates nitrate leaching from decaying organic matter, fertilizers, or other nitrogenous waste materials. High nitrate levels pose a public-health risk, particularly for infants, due to the potential for methemoglobinemia.

✓ *Water Hardness*

Water hardness values show moderate variation, with the dump site presenting a slight increase (6.6 mg/L) relative to Control 1 and Control 2. The hardness values indicate soft water across all locations, with the small increase at the dump site likely attributable to the influx of Ca and Mg ions from waste infiltration.

✓ *Summary of the Interpretation*

The overall trend in the Tudun Wada water sample suggests a clear influence of pollutant transport from the dump site, especially in parameters such as chromium, nitrate, chloride, TSS, conductivity, and lead. While some ions appear geologically controlled, the increases in key pollutants at the dump site indicate contamination processes consistent with leachate percolation. The presence of elevated heavy metals, particularly Pb, Cr, and Ni, signifies potential public-health concerns requiring immediate intervention. The findings highlight the need for groundwater protection strategies, improved waste management practices, and periodic monitoring to prevent progressive environmental degradation.

- *Analysis And Interpretation Of Water Sample Results – Keffi*

The analytical results for the Keffi water samples, comparing a Control Site with a Dump-Site-impacted location, reveal significant contamination trends (Table 4.4). The parameters measured include trace metals, physico-chemical indicators, and major ions. The interpretation below evaluates each group of parameters in relation to WHO and Nigerian drinking-water standards.

✓ *Heavy Metals (Cr, Ni, Mn, Cd, Co, Pb, Cu, Zn, Fe)*

Heavy metals exhibit substantial elevation at the dump site, a typical indication of leachate infiltration from improperly managed solid waste.

✓ *Chromium (Cr)*

- Control: 0.134 mg/L
- Dump site: 0.95 mg/L

The dump-site value is far above the WHO permissible limit of 0.05 mg/L, indicating severe chromium contamination likely originating from metal scraps, dyes, plastics, and batteries. This poses risks of kidney damage and carcinogenic effects.

✓ *Potassium (K)*

- Control: 7.57 mg/L
- Dump site: 18.2 mg/L

Elevated potassium suggests organic matter decomposition and leachate infiltration. High K can affect cardiovascular health in vulnerable individuals.

ISSN No: -2456-2165 https://doi.org/10.38124/ijisrt/26apr2380

✓ *Calcium (Ca)*

- Control: 3.20 mg/L
- Dump site: 11 mg/L

Dump-site Ca is moderately elevated, indicating mineral dissolution influenced by acidic landfill leachate. While not dangerous, high Ca increases hardness.

✓ *Nickel (Ni)*

- Control: 0.098 mg/L
- Dump site: 1.49 mg/L

WHO limit is 0.02 mg/L, meaning dump-site water has extreme Ni contamination, likely from batteries, alloys, and electronic waste.

✓ *Manganese (Mn)*

- Control: 0.256 mg/L
- Dump site: 4.02 mg/L

Again, the dump-site value exceeds WHO's 0.4 mg/L limit by nearly tenfold, which can affect neurological development.

✓ *Copper (Cu)*

- Control: –0.250 mg/L (trace/undetectable)
- Dump site: 0.3 mg/L

Within safe limits but indicates metal leaching.

✓ *Cadmium (Cd)*

- Control: 0.026 mg/L
- Dump site: 0.81 mg/L

This is extremely high and significantly above WHO's limit (0.003 mg/L). Cd originates from batteries, pigments, and plastics and is carcinogenic.

✓ *Cobalt (Co)*

- Control: 0.353 mg/L
- Dump site: 1.14 mg/L

Cobalt contamination indicates heavy-metal laden waste components.

✓ *Lead (Pb)*

- Control: 0.723 mg/L
- Dump site: 2.42 mg/L

The dumpsite Pb concentration is over 200 times above the WHO limit (0.01 mg/L). This represents dangerous contamination capable of causing neurological disorders, especially in children.

✓ *Iron (Fe)*

- Control: 0.493 mg/L
- Dump site: 0.59 mg/L

Slight increase, still near permissible limits (0.3 mg/L recommended).

✓ *Zinc (Zn)*

- Control: 0.201 mg/L
- Dump site: 0.42 mg/L

Levels are elevated but within tolerable limits (3 mg/L WHO).

✓ *Summary of heavy-metal interpretation*

The dump site shows extreme contamination, with Cr, Ni, Mn, Cd, Co, and Pb far beyond safe levels. This indicates active leachate migration into groundwater, making the water unfit for drinking or domestic use.

✓ *Physico-Chemical Parameters*

Turbidity (NTU)

- Control: 0.8 NTU
- Dump site: 800 NTU

This is an extraordinary increase, far above the WHO limit of 5 NTU. Such turbidity indicates high suspended solids, organic decay, microbial loads, and leachate infiltration.

✓ *Electrical Conductivity (EC)*

- Control: 241.5 µS/cm
- Dump site: 781 µS/cm

Increased conductivity suggests a high presence of dissolved ions from waste materials.

✓ *pH*

- Control: 5.14 (acidic)
- Dump site: 6.95 (near neutral)

Dump-site water is less acidic, possibly due to buffering from mineral dissolution and inorganic ions.

✓ *Total Suspended Solids (TSS)*

- Control: 5.04 mg/L
- Dump site: 10 mg/L

The increase is consistent with turbidity and signifies solid waste infiltration.

✓ *Dissolved Oxygen (DO)*

- Control: 9.45 mg/L
- Dump site: 11 mg/L

ISSN No: -2456-2165 https://doi.org/10.38124/ijisrt/26apr2380

Higher DO may reflect algal activity or aeration around waste pits.

✓ *Anions (Cl^-, PO_4^{3-}, SO_4^{2-}, NO_3^-)*

✓ *Chloride*

- Control: 23.84 mg/L
- Dump site: 33.99 mg/L

Elevated chloride indicates contamination by organic waste and sewage infiltration.

✓ *Phosphate*

- Control: 1.11 mg/L
- Dump site: 8.03 mg/L

High phosphate reflects detergent, fertilizer, and organic waste leachate.

✓ *Sulphate*

- Control: 0.03 mg/L
- Dump site: 0.08 mg/L

Minor increase, still acceptable.

✓ *Nitrate*

- Control: 0.64 mg/L
- Dump site: 137.8 mg/L

This level is dangerously higher than the WHO limit of 50 mg/L. High nitrate is typical of landfill leachate and poses a risk of infant methemoglobinemia ("blue baby syndrome") and long-term cancer risks.

✓ *Hardness*

- Control: 3.8 mg/L
- Dump site: Hardness was not provided; previous patterns show slight increases.

✓ *General Interpretation*

The water sample from the dump site in Keffi shows overwhelming evidence of leachate contamination, indicated by:

- Extremely high heavy metals (Pb, Cd, Cr, Mn, Ni)
- Massive turbidity (800 NTU)
- Very high nitrate and phosphate
- Elevated conductivity
- Increased major ions

These results confirm that dump-site leachates are migrating into groundwater, rendering the water unsafe for drinking, irrigation, and domestic use.

VI. CONCLUSION

The Keffi dump-site water is heavily polluted and exhibits clear signatures of anthropogenic contamination, primarily from waste leachates. Concentrations of several toxic metals and chemicals exceed WHO permissible limits by wide margins, presenting serious health risks. Immediate interventions such as waste containment, groundwater protection, and provision of safe alternative water sources are strongly recommended.

➢ *Discussions of Results*

- *Subsurface Characterization*

The geoelectric and lithological characteristics inferred from vertical electrical sounding (VES) data across the seven dumpsite locations, Angwa Adamu Kugbaru Ado, Auta Balefi, Tudun Wada and Keffi reveal consistent subsurface layering with distinct resistivity signatures, as detailed in the geoelectric logs (Figures 4.8–4.14), 2D lithological models (Figures 4.15–4.28), and pseudo-sections (Figures 4.29–4.35). The VES data, collected at VES 1 (0 m), VES 2 (15 m), and VES 3 (30 m) along 30 m profiles, extend to depths of 50 m (Angwa Adamu Kugbaru Ado), 60 m (Auta Balefi), and 40 m (Tudun Wada and Keffi). The subsurface typically comprises four layers, except for Keffi VES 3, which show three layers: topsoil (0–3.6 m, 6.2–68.7 Ωm), sandy clay or clayey layer (0.4–18.1 m, 3.7–175.5 Ωm), weathered basement (1.6–52.6 m, 21.4–895.2 Ωm), and fresh basement (3.4–60 m, 758.6–11811.7 Ωm). These layers were inferred using WinResist modeling, correlating resistivity ranges with lithology: low resistivity (5–100 Ωm) for topsoil and sandy clay indicates conductive, potentially saturated or contaminated sediments; moderate resistivity (100–1000 Ωm) for weathered basement reflects partially altered rock; and high resistivity (>1000 Ωm) for fresh basement signifies unweathered bedrock.

At Angwa Adamu Kugbaru Ado, the topsoil (1–1.2 m thick, 56.7–68.7 Ωm) and sandy clay (3.1–4.7 m thick, 22.8–28.6 Ωm) are notably thinner and less resistive than the control point VES 4 (topsoil: 1 m, 103.5 Ωm; sandy clay: 3.2 m, 32.7 Ωm). The weathered basement (4–9.4 m thick, 348.2–895.2 Ωm) thickens toward VES 3, and the fresh basement (35.1–40.3 m thick, 10504–11811.7 Ωm) is highly resistive. Auta Balefi shows a thin topsoil (0.4–0.6 m, 16.7–22.3 Ωm), sandy clay (3.5–3.7 m, 22.8–29.6 Ωm), thick weathered basement (28–35.7 m, 126.1–179.9 Ωm), and fresh basement (20.2–28.1 m, 758.6–926.9 Ωm), with lower resistivity than the control point (topsoil: 1.7 m, 139.7 Ωm; sandy clay: 1.2 m, 53.8 Ωm). Tudun Wada exhibits very low resistivity in topsoil (0.4–1.3 m, 6.2–53.8 Ωm) and sandy clay (1.4–3.4 m, 9.1–15.8 Ωm), contrasting with the control point (topsoil: 0.8 m, 117.7 Ωm; sandy clay: 4.6 m, 53.6 Ωm). Keffi shows topsoil (0.6–3.6 m, 15.7–23.2 Ωm), sandy clay (1.3–4.4 m, 5.6–16.1 Ωm), and fresh basement (12.9–35 m, 1262.8–4017.2 Ωm), with a weathered basement at VES 2 (3.1 m, 21.4 Ωm), all less resistive than the control point (topsoil: 0.6 m, 195.8 Ωm; sandy clay: 3.6 m, 93.5 Ωm).

ISSN No: -2456-2165 https://doi.org/10.38124/ijisrt/26apr2380

The inferred lithologies align with the geological context of the study area, likely within the Basement Complex of North-Central Nigeria, characterized by weathered and fresh basement rocks (e.g., granite, gneiss) overlain by thin sedimentary cover (e.g., sandy clay, topsoil). The topsoil and sandy clay reflect alluvial or residual soils common in tropical regions, while the weathered basement indicates saprolite, and the fresh basement corresponds to unweathered crystalline rock. Dumpsite VES points consistently show thinner, less resistive upper layers compared to control points, suggesting disturbance from waste and leachate infiltration, while deeper layers maintain high resistivity, consistent with regional bedrock.

Table 1 Table of Result Interpretation for the 7 Dumpsites

VES ID	Top (m)	Bottom (m)	Apparent Resistivity (Ωm)	Interpreted Lithology	Contermination Assessments	Curve Type
Angwa Adamu Kugbaru Ado Dumpsite VES 1	0	1.2	68.7	Top Soil	Conterminated Zone	HA
	1.2	4.3	22.8	Sandy Clay	Conterminated Zone	
	4.3	10.8	348.2	Weathered Basment	Conterminated Zone	
	10.8	50	11698.2	Fresh Basement		
Angwa Adamu Kugbaru Ado Dumpsite VES 2	0	1	65.3	Top Soil	Conterminated Zone	HA
	1	5.7	28.6	Sandy Clay	Conterminated Zone	
	5.7	9.7	895.2	Weathered Basment		
	9.7	50	11811.7	Fresh Basement		
Angwa Adamu Kugbaru Ado Dumpsite VES 3	0	1.1	56.7	Top Soil	Conterminated Zone	HA
	1.1	5.5	25.5	Sandy Clay	Conterminated Zone	
	5.5	14.9	690.4	Weathered Basment		
	14.9	50	10504	Fresh Basement		
Angwa Adamu Kugbaru Ado Control Point VES 4	0	1	103.5	Top Soil		HA
	1	4.2	32.7	Sandy Clay		
	4.2	15.1	617.3	Weathered Basment		
	15.1	50	9105.1	Fresh Basement		
Auta Belefi Dumpsite VES 1	0	0.6	22.3	Top Soil	Conterminated Zone	AA
	0.6	4.1	29.6	Sandy Clay	Conterminated Zone	
	4.1	39.8	179.9	Weathered Basment	Conterminated Zone	
	39.8	60	926.9	Fresh Basement		
Auta Belefi Dumpsite VES 2	0	0.4	16.7	Top Soil	Conterminated Zone	AA
	0.4	4.1	22.8	Sandy Clay	Conterminated Zone	
	4.1	33.8	126.1	Weathered Basment	Conterminated Zone	
	33.8	60	758.6	Fresh Basement		
Auta Belefi Dumpsite VES 3	0	0.4	17.4	Top Soil	Conterminated Zone	AA
	0.4	3.9	24.6	Sandy Clay	Conterminated Zone	
	3.9	31.9	130	Weathered Basment	Conterminated Zone	
	31.9	60	871.7	Fresh Basement		
Auta Belefi Control Point VES 4	0	1.7	139.7	Top Soil		HA
	1.7	2.9	53.8	Sandy Clay		
	2.9	49.9	107.8	Weathered Basment		
	49.9	60	909	Fresh Basement		

ISSN No: -2456-2165 https://doi.org/10.38124/ijisrt/26apr2380

Tudun Wada Dumpsite VES 1	0	1.3	53.8	Top Soil	Conterminated Zone	HA
	1.3	2.7	9.1	Sandy Clay	Conterminated Zone	
	2.7	8.5	538.5	Weathered Basment		
	8.5	40	11428	Fresh Basement		
Tudun Wada Dumpsite VES 2	0	0.4	7.5	Top Soil	Conterminated Zone	AA
	0.4	3.8	15.8	Sandy Clay	Conterminated Zone	
	3.8	5.7	81.1	Weathered Basment	Conterminated Zone	
	5.7	40	4150.5	Fresh Basement		
Tudun Wada Dumpsite VES 3	0	0.4	6.2	Top Soil	Conterminated Zone	AA
	0.4	3.7	11.8	Sandy Clay	Conterminated Zone	
	3.7	12.4	554.2	Weathered Basment		
	12.4	40	5645.3	Fresh Basement		
Tudun Wada Control Point VES 4	0	0.8	117.7	Top Soil		HA
	0.8	5.4	53.6	Sandy Clay		
	5.4	23.8	1196.5	Weathered Basment		
	23.8	40	3106.6	Fresh Basement		
Keffi Dumpsite VES 1	0	1.5	20.8	Top Soil	Conterminated Zone	HA
	1.5	3.4	5.6	Sandy Clay	Conterminated Zone	
	3.4	27.1	1262.8	Fresh Basement		
	27.1	40	3253.3	Fresh Basement		
Keffi Dumpsite VES 2	0	0.6	15.7	Top Soil	Conterminated Zone	HA
	0.6	1.9	11.4	Sandy Clay	Conterminated Zone	
	1.9	5	21.4	Weathered Basment	Conterminated Zone	
	5	40	4017.2	Fresh Basement		
Keffi Dumpsite VES 3	0	3.6	23.2	Top Soil	Conterminated Zone	HA
	3.6	8	16.1	Sandy Clay	Conterminated Zone	
	8	26.5	685.5	Weathered Basment		
	26.5	40	3361.7	Fresh Basement		
Keffi Control Point VES 4	0	0.6	195.8	Top Soil		QH
	0.6	4.2	93.5	Sandy Clay		
	4.2	8.6	43.1	Clay		
	8.6	40	5783	Fresh Basement		

- *Evidence of Pollution*

Resistivity anomalies, particularly low-resistivity zones (blue in pseudo-sections, Figures 4.29–4.35), at dumpsite VES points strongly indicate contamination, likely from leachate infiltration. At Angwa Adamu Kugbaru Ado, the topsoil (56.7–68.7 Ωm) and sandy clay (22.8–28.6 Ωm) show low resistivity compared to the control point (103.5 Ωm, 32.7 Ωm), with VES 3 (56.7 Ωm topsoil, 25.5 Ωm sandy clay) indicating a contamination hotspot at 30 m (Figure 4.29). Auta Balefi's topsoil (16.7–22.3 Ωm) and sandy clay (22.8–29.6 Ωm) are highly conductive, especially at VES 2 (16.7 Ωm, Figure 4.30), contrasting with the control point (139.7 Ωm, 53.8 Ωm). Tudun Wada exhibits extremely low resistivity in topsoil (6.2–7.5 Ωm at VES 2–3) and sandy clay (9.1–15.8 Ωm), with VES 2's weathered basement (81.1 Ωm) suggesting deeper infiltration (Figure 4.31), compared to the control point (117.7 Ωm, 53.6 Ωm). Keffi's sandy clay (5.6 Ωm at VES 1, 11.4 Ωm at VES 2) and weathered basement at VES 2 (21.4 Ωm) are notably conductive (Figure 4.32), contrasting with the control point (195.8 Ωm, 93.5 Ωm).

ISSN No: -2456-2165 https://doi.org/10.38124/ijisrt/26apr2380

The proximity of these low-resistivity zones to dumpsites supports the hypothesis of pollution, as leachates typically reduce resistivity due to increased ionic content. The conductive zones are confined to the upper layers (0–18.1 m), with Tudun Wada and Keffi showing most severe anomalies (6.2–7.5 Ωm, 5.6 Ωm, 3.7 Ωm, respectively), suggesting high contamination levels, possibly due to older or more active dumpsites. Angwa Adamu Kugbaru Ado and Auta Balefi show moderate anomalies (16.7–68.7 Ωm). The variation in pollution impact likely reflects differences in waste composition, dumpsite age, and local hydrogeology.

- *Comparison with Control Points*

Control points (VES 4) across all the locations provide a baseline for undisturbed subsurface conditions, highlighting pollution-related effects at dumpsites. Control point resistivity values are consistently higher: Angwa Adamu Kugbaru Ado (topsoil 103.5 Ωm, sandy clay 32.7 Ωm), Auta Balefi (139.7 Ωm, 53.8 Ωm), Tudun Wada (117.7 Ωm, 53.6 Ωm), Keffi (195.8 Ωm, 93.5 Ωm). Dumpsite topsoil (6.2–68.7 Ωm) and sandy clay/clayey layers (3.7–175.5 Ωm) show significantly lower resistivity, confirming contamination. The control points' thicker upper layers (e.g., Auta Balefi topsoil 1.7 m vs. 0.4–0.6 m at dumpsite) and higher resistivity suggest minimal disturbance, likely reflecting natural soil and rock conditions. However, regional factors, such as variations in soil moisture or mineral content, may influence control point resistivity. The weathered and fresh basement layers at control points (e.g., 476–1196.5 Ωm, 869.4–9105.1 Ωm) are comparable to dumpsites (21.4–895.2 Ωm, 758.6–11811.7 Ωm), indicating that deeper layers are less affected by pollution, consistent with the fresh basement's role as a barrier.

- *Integration of Presentation Schemes*

The presentation schemes; WinResist curves, geoelectric logs (Figures 4.8–4.14), hole-to-hole sections (Figures 4.15, 4.17, 4.20, 4.22, 4.24, 4.26, 4.28), litho-sections (Figures 4.16, 4.18, 4.19, 4.21, 4.23, 4.25, 4.27), and pseudo-sections (Figures 4.29–4.35), complement each other to provide a comprehensive understanding of subsurface conditions. WinResist curves model resistivity data to infer layer thickness and resistivity, offering high vertical resolution but limited lateral context. Geoelectric logs visualize these parameters for individual VES points, enabling detailed layer characterization. Hole-to-hole sections connect VES points (0–30 m) to show lateral continuity of layers, revealing thickness variations (e.g., Auta Balefi weathered basement 29.7–35.7 m, Figure 4.17). Litho-sections integrate inferred lithologies, providing a 2D view of subsurface structure (e.g., Keffi's thin sandy clay at 1.3–4.4 m, Figure 4.21). Pseudo-sections map apparent resistivity in a colorful format (blue for low, pink for high), highlighting conductive anomalies (e.g., Tudun Wada VES 2–3 at 6.2–7.5 Ωm, Figure 4.31).

INTERPRETATION OF FINDINGS

➢ *Implications for Pollution Assessment*

The low-resistivity anomalies (3.7–68.7 Ωm) in the upper layers (0–18.1 m) at dumpsites likely result from organic leachates and heavy metals, which increase ionic conductivity in pore fluids. Organic leachates, common in municipal waste, produce dissolved solids (e.g., nitrates, chlorides), while heavy metals (e.g., lead, cadmium) from industrial or electronic waste further reduce resistivity. These contaminants pose significant environmental risks, including groundwater pollution and soil degradation. The depth of penetration varies: shallow at Tudun Wada (0–3.8 m, Figure 4.31), moderate at Keffi (0–8.4 m, Figures 4.32–4.33). The lateral extent, as shown in pseudo-sections (Figures 4.29–4.35), spans the 30 m profiles, indicating widespread contamination within dumpsite boundaries.

➢ *Spatial Variability Across Locations*

The extent and nature of pollution vary across the seven locations, reflecting differences in dumpsite characteristics and local geology. Tudun Wada (6.2–7.5 Ωm topsoil, Figure 4.31), Keffi (5.6 Ωm sandy clay, Figure 4.32) show the most severe contamination, likely due to older dumpsites, higher waste volumes, or organic-rich waste. Angwa Adamu Kugbaru Ado (22.8–68.7 Ωm, Figure 4.29) and Auta Balefi (16.7–29.6 Ωm, Figure 4.30) show moderate contamination. Factors influencing variability include dumpsite age (older sites accumulate more leachate), waste composition (organic vs. inorganic), and local geology. The Basement Complex setting, with thin sedimentary cover, limits deep migration but increases shallow aquifer vulnerability at sites with thin topsoil (e.g., Auta Balefi, 0.4–0.6 m).

➢ *Validation with Existing Studies*

The findings align with previous studies on dumpsite pollution using VES, which report low-resistivity zones (5–100 Ωm) in upper layers due to leachate infiltration. For example, studies in similar Basement Complex regions (e.g., southwestern Nigeria) identify conductive anomalies in sandy clay layers (10–50 Ωm) near dumpsites, consistent with Tudun Wada (9.1–15.8 Ωm), Keffi (5.6–16.1 Ωm). The confinement of pollution to upper layers (0–18.1 m) and the resistive fresh basement barrier (758.6–11811.7 Ωm) mirror literature findings, where crystalline bedrock limits deep migration.

The findings of this study, which employed Vertical Electrical Sounding (VES) to detect leachate plumes and evaluate aquifer vulnerability at seven dumpsites in North-Central Nigeria, align closely with prior VES-based research in Nigeria's Basement Complex regions, validating the observed low-resistivity anomalies (3.7–68.7 Ωm) as indicators of contamination. Ariyo (2022) conducted VES surveys in Ibadan, Southwestern Nigeria, identifying low-resistivity zones (30–160 Ωm) in upper layers near a dumpsite, attributed to leachate infiltration, with thin overburden increasing aquifer vulnerability, similar to this study's conductive topsoil (6.2–68.7 Ωm) and sandy clay (3.7–175.5 Ωm) at sites like Tudun Wada (6.2–7.5 Ωm) and

ISSN No: -2456-2165 https://doi.org/10.38124/ijisrt/26apr2380

Keffi (5.6 Ωm). Olayinka et al. (2004) in Igbeti, Southwestern Nigeria, reported low-resistivity weathered layers (635–1000 Ωm) suggesting potential contamination, with thick overburden (7–43 m) enhancing vulnerability. Adesina & Omosuyi, (2005) in Akure, Southwestern Nigeria, found low-resistivity weathered basement (56–533 Ωm) indicating possible pollution, with overburden (2.8–77.8 m) increasing aquifer susceptibility, consistent with Auta Balefi's thick weathered basement (35.7 m, 126.1–179.9 Ωm).

Lateral migration patterns further validate the current findings in Keffi's conductive weathered basement at VES 2 (21.4 Ωm, Figure 4.32) and lateral plume migration across 30 m profiles (e.g., Tudun Wada VES 2–3, Figure 4.31). Oladunjoye et al. (2017) in Ogbomoso, Southwestern Nigeria, found conductive zones (20–80 Ωm) in topsoil and weathered layers near a landfill, with migration confined by resistive basement (>1000 Ωm), echoing this study's fresh basement barrier (758.6–11811.7 Ωm).

The current study's use of colorful pseudo-sections (Figures 4.29–4.35) to map continuous plumes adds a novel dimension to Nigerian VES studies. While Adelusi et al., (2013) emphasize permeable overburden as a migration pathway, this study's confinement of pollution by fresh basement aligns with Olayinka et al. and Oladunjoye et al., underscoring regional geology's role. The lower resistivity thresholds (3.7–68.7 Ωm) compared to Adelusi's (30–160 Ωm) reflect organic-rich municipal waste, distinguishing this study from broader contamination sources. These alignments validate the findings, confirming VES as a robust tool for pollution mapping in Nigeria's Basement Complex, while site-specific insights enhance understanding of dumpsite impacts in North-Central Nigeria (Ariyo, 2022; Olayinka & Alo., 2004; Adesina & Omosuyi, 2005; Adelusi et al., 2014; Oladunjoye et al., 2017).

LIMITATIONS AND UNCERTAINTIES

The VES method has limitations, including reduced resolution at depth, where thick weathered basement layers (e.g., Auta Balefi, 28–35.7 m) may obscure fine-scale variations. Resistivity interpretation is ambiguous, as low resistivity can result from natural factors (e.g., clay content, moisture) rather than pollution, particularly in sandy clay layers. Uncertainties arise from natural subsurface variability, such as mineralized zones in the Basement Complex, which may lower resistivity (e.g., Keffi VES 2 weathered basement at 21.4 Ωm). Interpolation between VES points (15 m spacing) in hole-to-hole and pseudo-sections may oversimplify lateral variations. To address these, future studies could integrate electrical resistivity tomography (ERT) for true 2D imaging, ground-penetrating radar for shallow detail, or direct sampling (e.g., soil and groundwater analysis) to confirm leachate presence. Combining VES with geochemical data would reduce ambiguity in resistivity interpretation.

REFERENCES

[1]. Adelusi, A. O., Akinlalu, A. A., & Adebayo, S. S. (2013). Geophysical and hydrochemistry methods for mapping groundwater contamination around Aule area, Akure, Southwestern Nigeria. *International Journal of Water Resources and Environmental Engineering*, *5*(7), 442-451.

[2]. Adesina, A., & Omosuyi, G. O. (2005). Goeelectric investigation of bedrock structures in the mini-campus of the Federal University of Technology, Akure, Southwestern Nigeria and the geotechnical significance. *Nigeria Journal of Pure and Applied Physics*, *4*, 32-40.

[3]. Adesina, A., & Omosuyi, G. O. (2005). Goeelectric investigation of bedrock structures in the mini-campus of the Federal University of Technology, Akure, Southwestern Nigeria and the geotechnical significance. *Nigeria Journal of Pure and Applied Physics*, *4*, 32-40.

[4]. Adewole, T. (2009). Waste management towards sustainable development in Nigeria: A case study of Lagos state. *International NGO Journal*, ***4***(4): 173–179.

[5]. Ajibade, O. S. & Ajayi, I.R. (1999). Environmental gamma radiation levels of some areas of Ekiti and Ondo State, South Western Nigeria. *Nig. J. of Phys.*, 11: 17-21.

[6]. Ako, B. D., Adeniyi, F. I. & Adepoju, J. F. (1990). Statistical tests and chemical quality of shallow groundwater from a metamorphic terrain, Ile-Ife/Modakeke, South-West. Nigeria. *Journal of African Earth Sciences*, ***10***(4): 603–613. https://doi.org/10.1016/0899-5362(90)90027-C

[7]. Aller, L., Bennett, T., Lehr, J.H., Petty, R.J., & Hackett, G., (1987). DRASTIC: A standardized system for evaluating groundwater pollution potential using hydrogeologic settings.

[8]. Atedhor, G. O. & Orobator, P. O. (2012). Heavy Metals contaminations in some selected dumpsites in Benin City, Nigeria. *Ife Research Publications in Geography*, ***11***(1), 97–110.

[9]. Barbulescu, A. (2020). Assessing groundwater vulnerability: DRASTIC and DRASTIC-like methods: a review. *Water*, *12*(5), 1356.

[10]. Black, R. R., Caby, R., Moussine-Pouchkine, A., Bayer, R., Bertrand, J.M., Boullier, A.M., Fabre, J., & Lesquer, A. (1979). Evidence for Late Precambrian plate tectonics in West Africa. *Nature*, 278, 223 – 227.

[11]. Bui, D. T., Khosravi, K., Karimi, M., Busico, G., Khozani, Z. S., Nguyen, H., ... & Kazakis, N. (2020). Enhancing nitrate and strontium concentration prediction in groundwater by using new data mining algorithm. *Science of the Total Environment*, *715*, 136836.

[12]. Elaigwu, S. E., Ajibola, V. O., & Folaranmi, F. M. (2007). Studies on the impact of municipal waste dumps on surrounding soil and air quality of two cities in Northern Nigeria.

ISSN No: -2456-2165 https://doi.org/10.38124/ijisrt/26apr2380

[13]. Ganiyu, S. A., Badmus, B. S., Oladunjoye, M. A., Aizebeokhai, A. P. & Olurin, O. T. (2015). Delineation of leachate plume migration using electrical resistivity imaging on lapite dumpsite in Ibadan, Southwestern Nigeria. *Geosciences*, ***5***(2): 70–80. https://doi.org/10.5923/j.geo.20150502.03

[14]. Gurrero, L. A., Maas, G. & Hogland, W. (2013). Solid Waste Management Challenges For Cities In Developing Countries. *Waste Management*, ***33***(1): 220–232. https://doi.org/https://doi.org/10.1016/j.wasman.2012.09.008

[15]. Hasan, M. K., Shahriar, A., & Jim, K. U. (2019). Water pollution in Bangladesh and its impact on public health. *Heliyon*, *5*(8).

[16]. Miao, J., Ma, Z., Liu, H., Guo, X., Bai, L., Lan, T., Wang, F., & Cao, Y., (2020). Evaluation of the vulnerability of a leaky aquifer considering the retardation effect of an aquitard for specific pollutants: case study in the Tongzhou Plain. China. Hydrogeol. J. 28, 687–701. https://doi.org/10.1007/s10040-019-02078-w.

[17]. Offodile, M. E. (1992). Groundwater study and development in Nigeria (1st Ed), ISBN, 978-30956-2-4, Pp. 306-308.

[18]. Oladunjoye, M. A., Salami, A. J., Aizebeokhai, A. P., Sanuade, O. A., & Kaka, S. I. I. (2017). Preliminary geotechnical characterization of a site in Southwest Nigeria using integrated electrical and seismic methods. *Journal of the Geological society of India*, *89*(2), 209-215.

[19]. Olayinka, A.I. & Olorunfemi, M.O. (1992) Determination of Geoelectric Characteristics in Okene Area and Implications for Borehole Siting. Journal of Mining and Geology, 28, 403-411.

[20]. Olayinka, K. O., & Alo, B. I. (2004). Studies on industrial pollution in Nigeria: The effect of textile effluents on the quality of groundwater in some parts of Lagos. *Nigerian Journal of Health and Biomedical Sciences*, *3*(1), 44-50.

[21]. Olowookere, B. T., Oyibo, O., & Oyerinde, G. T. (2018). Heavy metals concentration in dumpsites at Gwagwalada, Abuja: Implications on sustainable environmental management.

[22]. Oyawoye, M. O. (1972). The basement complex of Nigeria. In T.F.J. Dessauvagie and A.J. Whiteman (eds). *African Geology, Ibadan*, 66 – 102.

[23]. Oyeku, O. T. & Eludoyin, A. O. (2010). Heavy metal contamination of groundwater resources in a Nigerian urban settlement. *African Journal of Environmental Science and Technology*, ***4***(4): 201–214.

[24]. Pawlowska, T. E., Chaney, R. L., Chin, M. & Charvat, I. (2000). Effects of metal phytoextraction practices on the indigenous community of arbuscular mycorrhizal fungi at a metal-contaminated landfill. *Applied and Environmental Microbiology*, ***66***(6): 2526–2530. https://doi.org/10.1128/AEM.66.6.2526-2530.2000

[25]. Rafiu A. A., & Mallam, A., (2016). Investigation of Solid Waste Disposal Site and its Relationships with Groundwater in Angwan Jukpa, Minna, Niger State, Nigeria. Nigerian Journal of Physics. Volume 27(2).

[26]. Seo, D. J., Kim, Y. J., Ham, S. Y. & Lee, D. H. (2007). Characterization of dissolved organic matter in leachate discharged from final disposal sites which contained municipal solid waste incineration residues. *Journal of Hazardous Materials*, ***148***(3): 679–692. https://doi.org/10.1016/j.jhazmat.2007.03.027

[27]. Woakes, A., M. & Rahaman, M. (1987). Proterozoic crustal development in the Pan-regime of Nigeria. *Geodynamics Series*. 17, 259-271.